Tokyo Institute of Technology
12th October 2016

Anomalous spin and flavor effects in high energy reactions

Nikolai Kochelev

Bogoliubov Laboratory of Theoretical Physics
Joint Institute for Nuclear Research,

Dubna, Russia

CONTENTS

- Instanton induced quark-quark, quark-gluon and quark-gluon-pion interactions
- Nonperturbative QCD dynamics in the elastic PP and $P\bar{P}$ scattering
- "Direct" meson production induced by the instanton gluon fields
- Nonperturbative energy loss by fast parton in Quark-Gluon Plasma
- Gluonic structure of constituent quark
- Flavor asymmetry in quark sea induced by instantons
- Instantons and anomalous single-spin asymmetries (SSA) in high energy reactions with hadrons
- Conclusion

Instanton induced quark-quark, quark-gluon and quark-gluon-pion interactions

QCD vacuum is not an empty space. It is a system of strong fluctuations of gluon fields called instantons

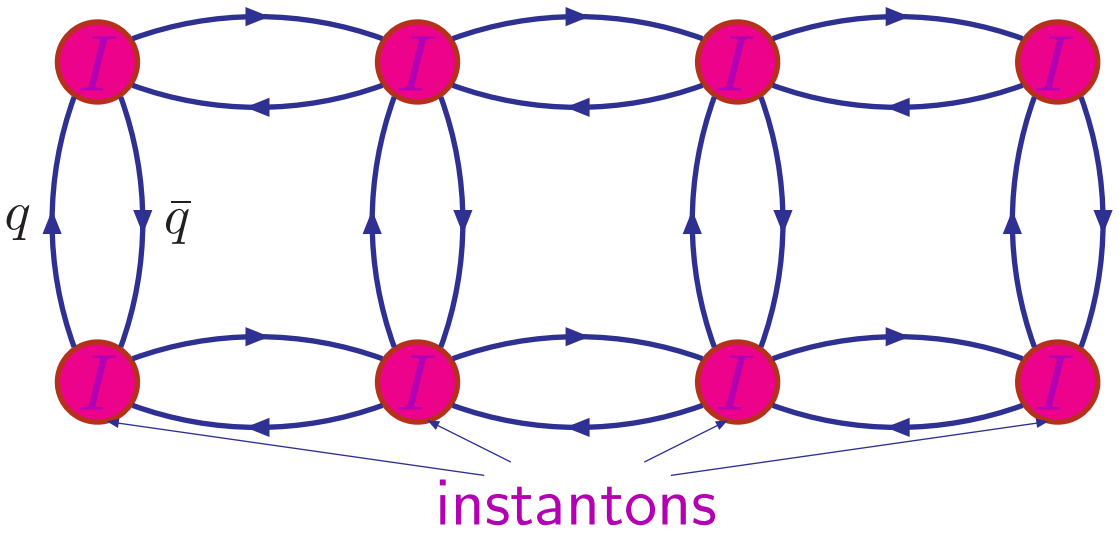

QCD vacuum structure is nontrivial: it is filled with instantons; quarks jump between them.

Analogy with the solid state

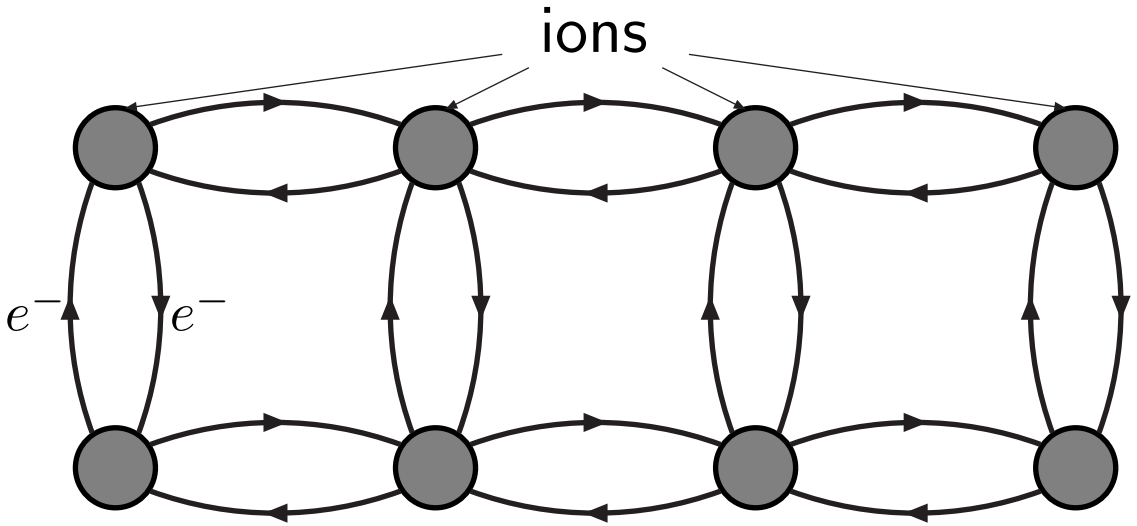

Two types of interaction:
1) Direct "perturbative" photon exchange.
2) "Non-perturbative" interaction through lattice (phonon exchange).

Discovery of instantons (1975) $\rightarrow$ Instanton liquid model (1982)

The model describes the QCD vacuum as a system of instantons and antiinstantons [Callan, Dashen, Gross, Shuryak, ...]

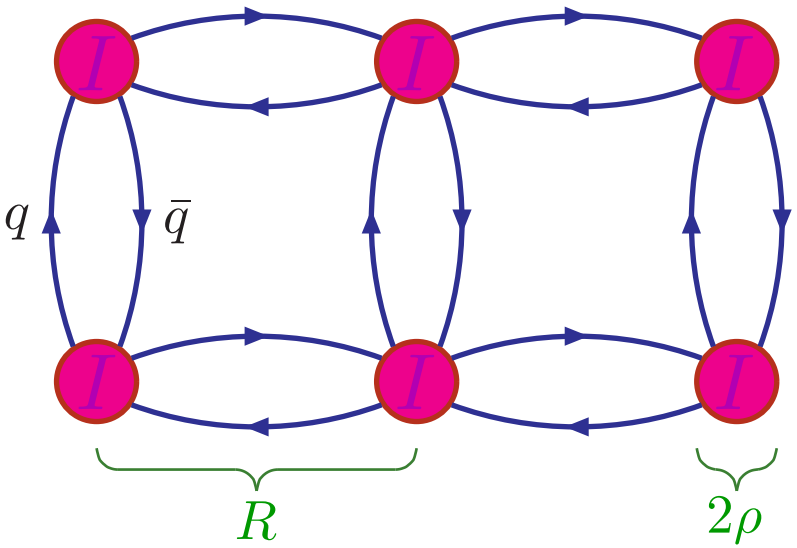

One can introduce the "density" of instantons

$$n_I(\rho) \sim exp\left(-\frac{2\pi}{\alpha_s(\rho)}\right)$$

R - distance between instantons

$\rho \approx 0.3$ fm - instanton size

If $R >> \rho \rightarrow$ vacuum is a "gas" of instantons

If $R \approx 3\rho \rightarrow$ vacuum is an instanton "liquid"

Instantons in $q-q$ and $q-g$ interactions

Quark-quark interaction [t'Hooft, 1976]

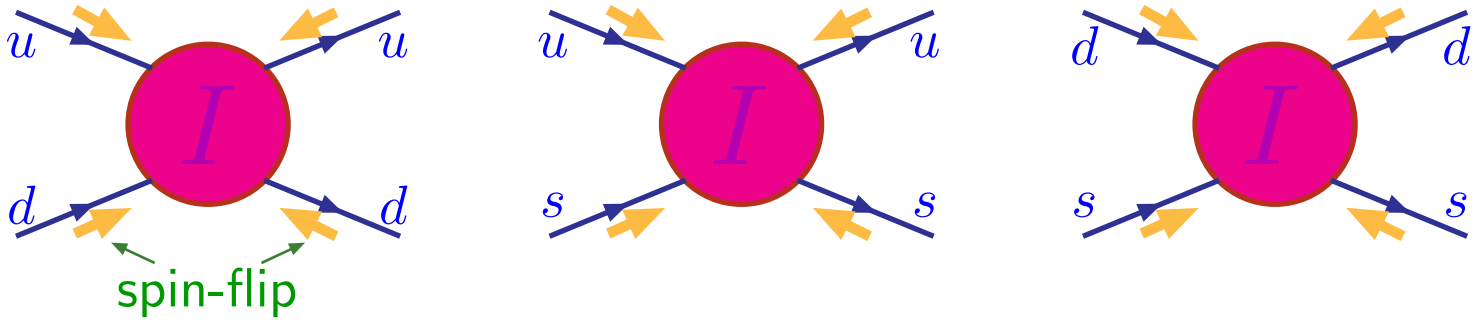

$$V_{q_i q_j}^{inst} = \sum_{i \neq j} \frac{\lambda}{m_i^* m_j^*} \left\{ 1 + 3\lambda_i^a \lambda_j^a \vec{\sigma}_i \vec{\sigma}_j \right\}$$

Features:

1) Non-zero only for different quark flavors

2) Quark spin-flip differs from the perturbative one gluon exchange

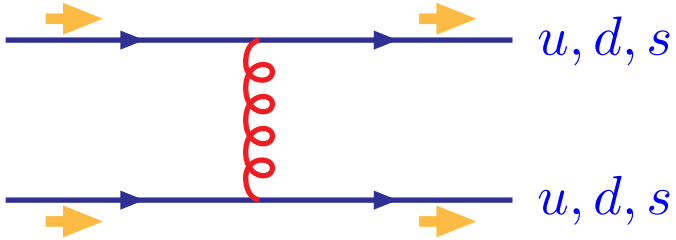

$$V_{q_i q_j}^{OGE} = \sum_{i,j} \frac{\lambda'}{m_i^* m_j^*} \lambda_i^a \lambda_j^a \vec{\sigma}_i \vec{\sigma}_j$$

Multiquark interactions induced by instantons

For N_f=3, $q = u, d, s \Rightarrow$ six-quark effective interaction induced by instantons

In $m_u = m_d = m_s \to 0$ limit

$$H_{t'Hooft} = \int d\rho n(\rho) \left(4\pi^2\rho^3\right)^3 \frac{1}{6N_C(N_C^2-1)} \varepsilon_{f_1 f_2 f_3} \varepsilon_{g_1 g_2 g_3} \times$$

$$\times \left\{ \frac{2N_C+1}{2N_C+4} \bar{q}_R^{f_1} q_L^{g_1} \bar{q}_R^{f_2} q_L^{g_2} \bar{q}_R^{f_3} q_L^{g_3} + \right.$$

$\frac{1}{N_C}$correction

$$\left. + \frac{3}{8(N_C+2)} \bar{q}_R^{f_1} q_L^{g_1} \bar{q}_R^{f_2} \sigma_{\mu\nu} q_L^{g_2} \bar{q}_R^{f_3} \sigma_{\mu\nu} q_L^{g_3} + (R \leftrightarrow L) \right\}$$

Very important in some processes: $K \to \pi\pi$ decays, $\Delta I = 1/2$ rule, CP violation, etc ..

Quark-gluon interactions induced by instantons

Anomalous quark-gluon chromomagnetic moment [N.K. Phys.Lett.B426 (1998) 149]

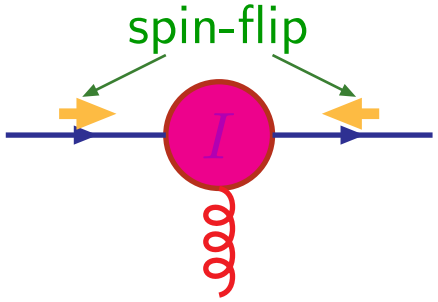

$$\Delta\mathcal{L} = -\imath\mu_a \frac{g_s}{2m_q^*}\bar{q}\sigma_{\mu\nu}t^a q G^a_{\mu\nu}$$

$\mu_a \approx -0.2$ [N.K. 1998]

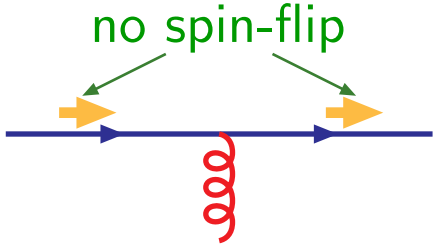

pQCD quark-gluon vertex

$$\Delta\mathcal{L} = g_s\bar{q}\gamma_\mu t^a q A^a_\mu$$

Spin-spin quark interaction induced by anomalous quark chromomagnetic moment

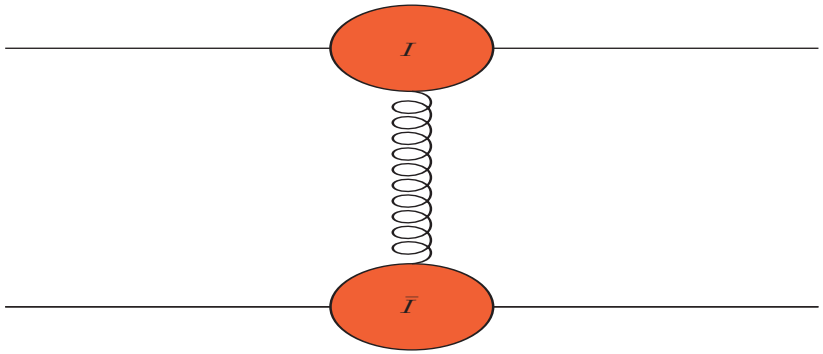

Figure 1: AQCM contribution to quark-quark scattering.

Instanton effects in high energy reactions

- **Anomalous quark-gluon and quark-gluon-pion interactions induced by instantons**

- In the general case, the interaction vertex of massive quark with gluon can be written in the following form:

$$V_\mu(k_1^2, k_2^2, q^2)t^a = -g_s t^a[\gamma_\mu F_1(k_1^2, k_2^2, q^2) + \frac{\sigma_{\mu\nu}q_\nu}{2M_q}F_2(k_1^2, k_2^2, q^2)],$$

where $k_{1,2}^2$ are virtualities of incoming and outcoming quarks and q is momentum transfer. It is similar to the photon-nucleon vertex

$$\Gamma_\mu{}^{QED} = \gamma_\mu F_1(q^2) + \frac{\sigma_{\mu\nu}q_\nu}{2M_N}F_2(q^2),$$

where $F_1(q^2), F_2(q^2)$ are Dirac and Pauli nucleon form factors, correspondently.

- Anomalous quark chromomagnetic moment (AQCM):

$$\mu_a = F_2(0, 0, 0).$$

$$\Delta\mathcal{L} = -\imath\mu_a \frac{g_s}{4M_q}\bar{q}\sigma_{\mu\nu}t^a q G^a_{\mu\nu}$$

The shape of form factor $F_2(k_1^2, k_2^2, q^2)$ within instanton model is fixed:

$$F_2(k_1^2, k_2^2, q^2) = \mu_a \Phi_q(\mid k_1 \mid \rho/2)\Phi_q(\mid k_2 \mid \rho/2)F_g(\mid q \mid \rho) \ ,$$

where

$$\begin{aligned} \Phi_q(z) &= -z\frac{d}{dz}(I_0(z)K_0(z) - I_1(z)K_1(z)), \\ F_g(z) &= \frac{4}{z^2} - 2K_2(z) \end{aligned}$$

are the Fourier-transformed quark zero-mode and instanton fields, respectively, and $I_\nu(z)$, $K_\nu(z)$,are the modified Bessel functions and ρ is the instanton size.

The value of AQCM is determined by the effective density of the instantons $n(\rho)$ in nonperturbative QCD vacuum (N.K. (1996))

$$\mu_a = -\pi^3 \int \frac{d\rho n(\rho)\rho^4}{\alpha_s(\rho)}.$$

Within Shuryak's instanton liquid model the relation between AQCM and dynamical quark mass is

$$\mu_a = -\frac{3\pi(M_q\rho_c)^2}{4\alpha_s(\rho_c)},$$

where $\rho_c \approx 0.3$ fm and $\alpha_s(\rho_c) \approx 0.5$.

The result is in very large AQCM $\mu_a \approx 0.2$ induced by nonperturbative QCD dynamics!

Quark-gluon-pion anomalous chromomagnetic interaction

$1/N_c$ correction to AQCM quark-gluon interaction-PCAC (Partially Conserved Axial Current) requirement. Lagrangian of σ model (pion part) from t'Hooft interaction (Diakonov,Petrov etc.):

$$\mathcal{L}_{eff} = \bar{q}[i\hat{\partial} - M_q e^{i\gamma_5\vec{\tau}\vec{\pi}/F_\pi}]q$$

Including AQCM effect gives the effective quark-gluon-pion interaction

(Polyakov, Diakonov 2003):

$$\Delta\mathcal{L}_{eff} = -\imath\mu_a \frac{g_s}{4M_q}\bar{q}\sigma_{\mu\nu}e^{i\gamma_5\vec{\tau}\vec{\pi}/F_\pi}t^a q G^a_{\mu\nu}$$

Nonperturbative QCD dynamics in the elastic PP and $P\bar{P}$ scattering

Included into current and future accelerator programs: NICA (Russia), J-PARC (Japan), PAX (FAIR,Germany), TOTEM (LHC, CERN).

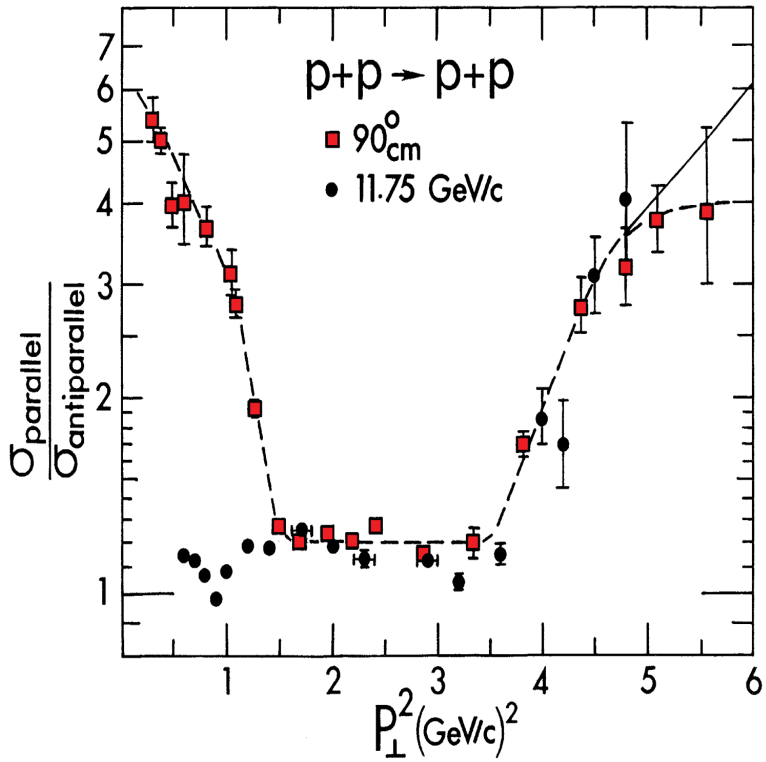

Figure 2: The measured spins-parallel / spins-antiparallel elastic cross-section ratio ($\sigma_{\uparrow\uparrow}/\sigma_{\uparrow\downarrow}$) plotted vs. P_t^2 (from A.D.Krisch, arXiv:1001.0790).

Pomerons and Odderon

- Two types of Pomerons:

- a) "Soft" Pomeron (quark virtuality is small):Intermediate spin-flip chromomagnetic interaction induced by vacuum gluonic instanton field. For heavy quarks there is suppression $1/{m_q}^2$.

- b) "Hard" Pomeron (quark virtuality is large): No spin-flip in intermediate state. There is no suppression for heavy quarks.

Odderon properties

Within the conventional approach, the Odderon P=C=-1 partner of Pomeron, originates from three gluon exchange with non-spin-flip perturbative-like quark-gluon vertex. The experimental support of the existence of such exchange comes from high energy ISR data on the difference in the dip structure around $\mid t \mid \approx 1.4$ GeV between the proton-proton and proton-antiproton differential cross section. However, there is no any signal for the Odderon at very small transfer momentum t.

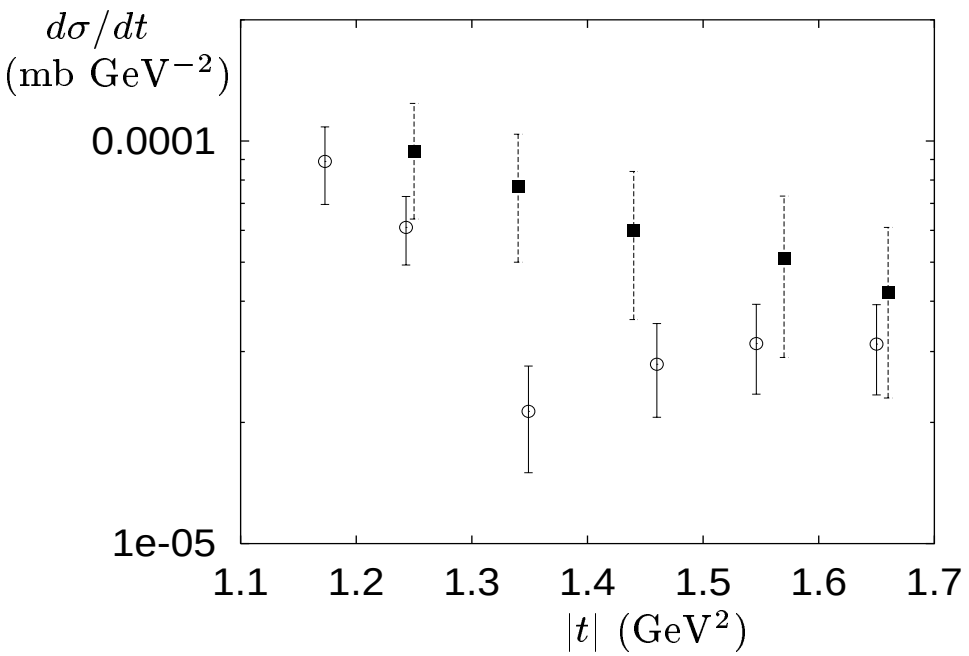

Figure 3: pp(lower points) and $\bar{p}p$(upper points) differential cross sections at $\sqrt{s} = 53$ GeV.

Quark-counting rule and Landshoff mechanism for elastic hadron-hadron scattering at large momentum transfer

• **Quark-counting rule (Matveev, Muradyan, Tavkelidze and Brodsky, Farrar (1973)) Differential cross-section for the scattering $AB \to CD$ at large S and $-t$ and $S \sim -t$ depends on the total number of valence quark in hadrons**

$$\frac{d\sigma}{dt} \sim s^{-n} f(\Theta)$$

where $n = n_A + n_B + n_c + n_D - 2$ and Θ is c.m. scattering angle. It comes from consideration of pQCD *connected* graphs.
For $PP \to PP$ $n = 10$ (fixed target experiment at AGS at low energy $p = 5.9$ GeV/c gives $n = 9.1 \pm 0.2$)

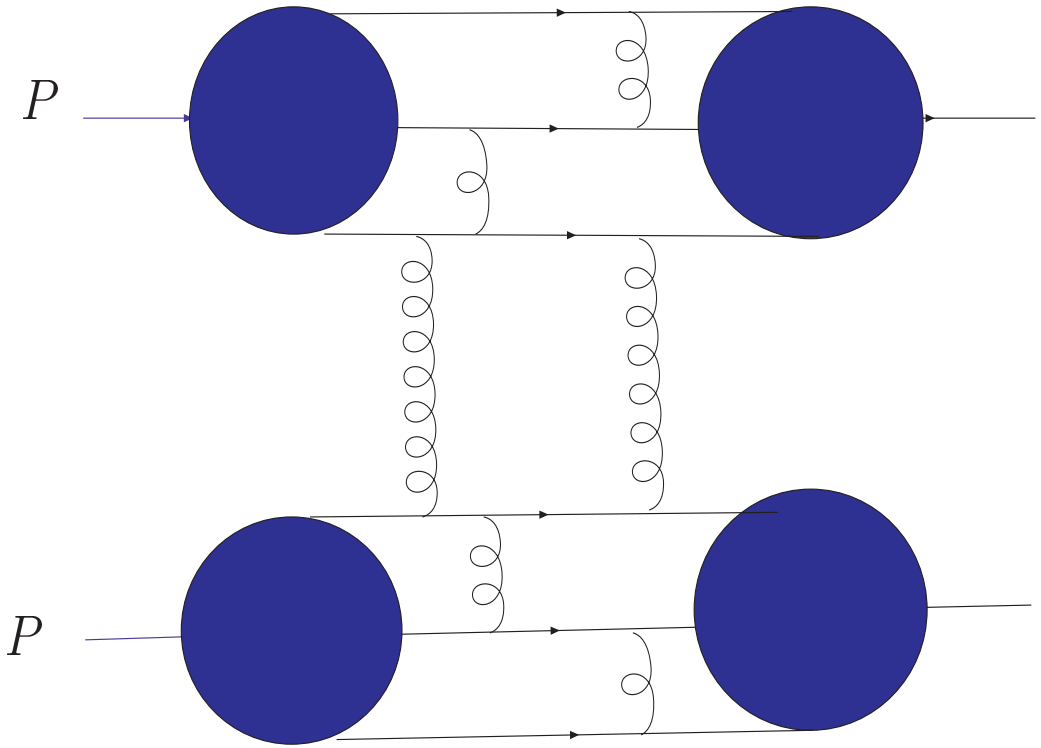

Figure 4: The example of pQCD contribution coming from the connected diagrams to the PP elastic scattering which leads to the quark-counting rule.

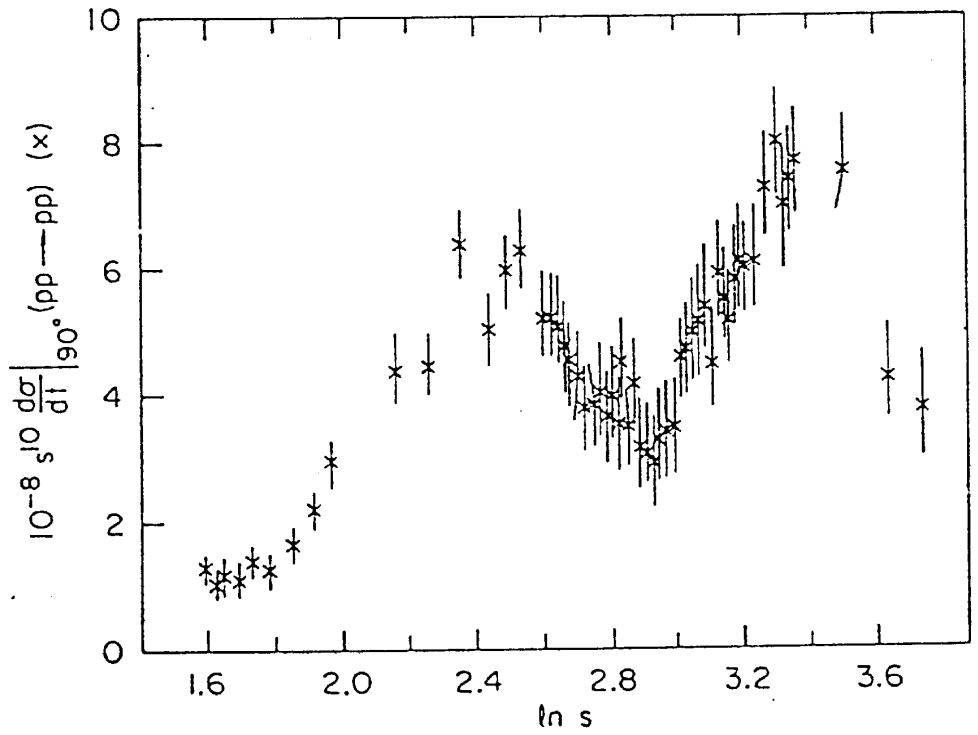

Figure 5: Deviation from quark-counting rule for differential cross-section of elastic PP scattering at 90° as the function of the energy (from Sivers et. al. Phys.Rep. **23** (1976) 1).

Landshoff's perturbative and nonperturbative mechanism for elastic hadron-hadron scattering at large momentum transfer

At large $S \gg -t$ and large $-t \gg M_P^2$ the differential cross section of PP and $P\bar{P}$ $d\sigma/dt$ does not depend on the energy.

Landshoff mechanism for large $q^2 = -t$ hadron-hadron scattering-contribution from disconnected diagrams (each gluon carries about $q/3$ transfer momentum).

Donnachie, Landshoff Z.Phys. C2 (1979)55 (D-L model)

According to our model, the perturbative part of the Odderon in the region of momentum transfer $on\ quark\ level!$ $p_\perp^{qq} \leq 3$ GeV ($-t^{qq} \leq 9$ GeV^2) is expected to be much smaller in comparison with the nonperturbative AQCM part. Elastic $PP \to PP$ at large $-t \geq 3$ GeV^2 in D-L model.

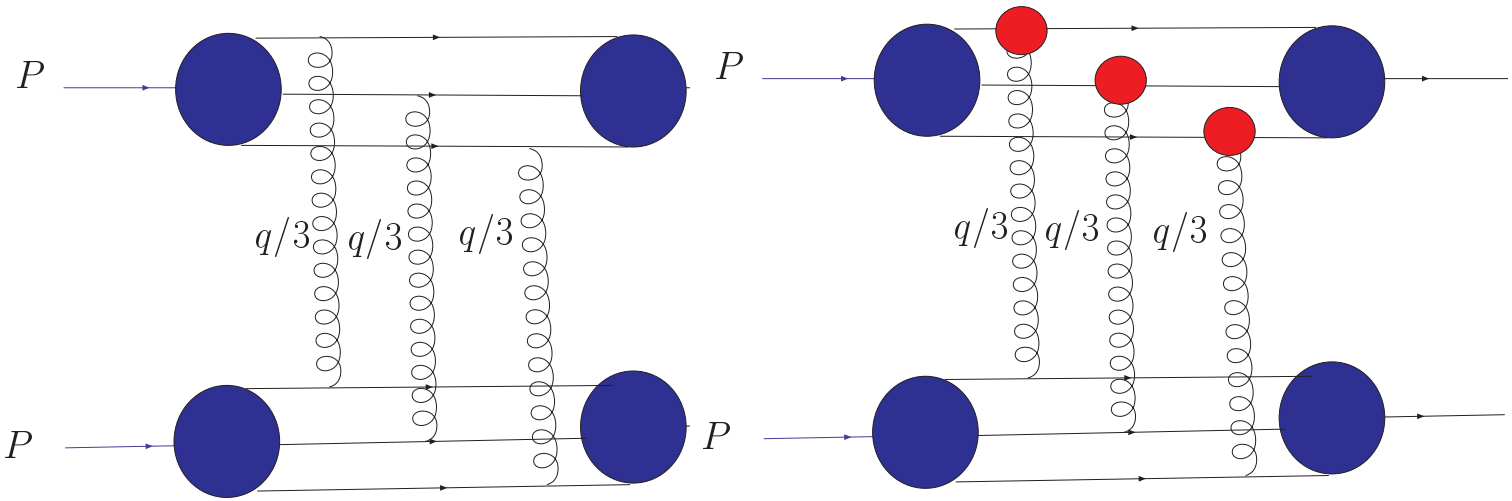

Figure 6: The left panel is Landshoff mechanism for large $-t$ nucleon-nucleon scattering. The right panel is an example of AQCM contribution.

$$\frac{d\sigma}{dt} \sim \frac{244P^4}{S^6t^2R^{12}} \mid M_{qq}(\Theta) \mid^6 \sim \frac{1}{t^2(t^2)^3} \sim \frac{1}{t^8},$$

where $S = (p_1 + p_2)^2$ and t is transfer momentum, P^2 is probability of

three quark configuration in proton and R is proton radius.

$$\mid M_{qq}^{pQCD}(\Theta) \mid^2 = \frac{128\pi^2\alpha_s^2}{9}\frac{\hat{s}^2}{\hat{t}^2},$$

where on the quark level $\hat{s} \approx S/9$, $\hat{t} \approx t/9$
and at $\hat{s} >> -\hat{t}$ $\hat{s}/\hat{t} \sim -4/sin^2(\Theta)$. In D-L estimation they use $ad\ hoc$:
$P = 1/10$, $\alpha_s = 0.3$ and $R^{-1} = 640$ MeV.
Very small proton radius $R \approx 0.3fm$!
If we take $P = 1$ and $R = 1$ fm we have got for $\alpha_s = 0.3$ $d\sigma/dt \sim 8 \cdot 10^{-4}/t^8$ mb/GeV^2 (two orders of magnitude less than the experiment: $\approx 9 \cdot 10^{-2}/t^8$ mb/GeV^2.)
AQCM contribution:

$$\begin{aligned}\mid M_{qq}^{AQCM}(S,t) \mid^2 &= \frac{4\pi^4 \mid \mu_a \mid \alpha_s(\mid \hat{t} \mid)}{9\alpha_s(\rho_c)}\frac{S^2}{\mid t \mid}(M_q\rho_c)^2\rho_c^2F_g^2(\sqrt{\mid t \mid}\rho_c/3) \\ &\quad +9\pi^4\mu_a^2\rho_c^4S^2F_g^4(\sqrt{\mid t \mid}\rho_c/3),\end{aligned}$$

Inspite of the fact that AQCM contribution asymptotically decays as $1/t^{11}$ it describes the existent large $-t$ data very well.

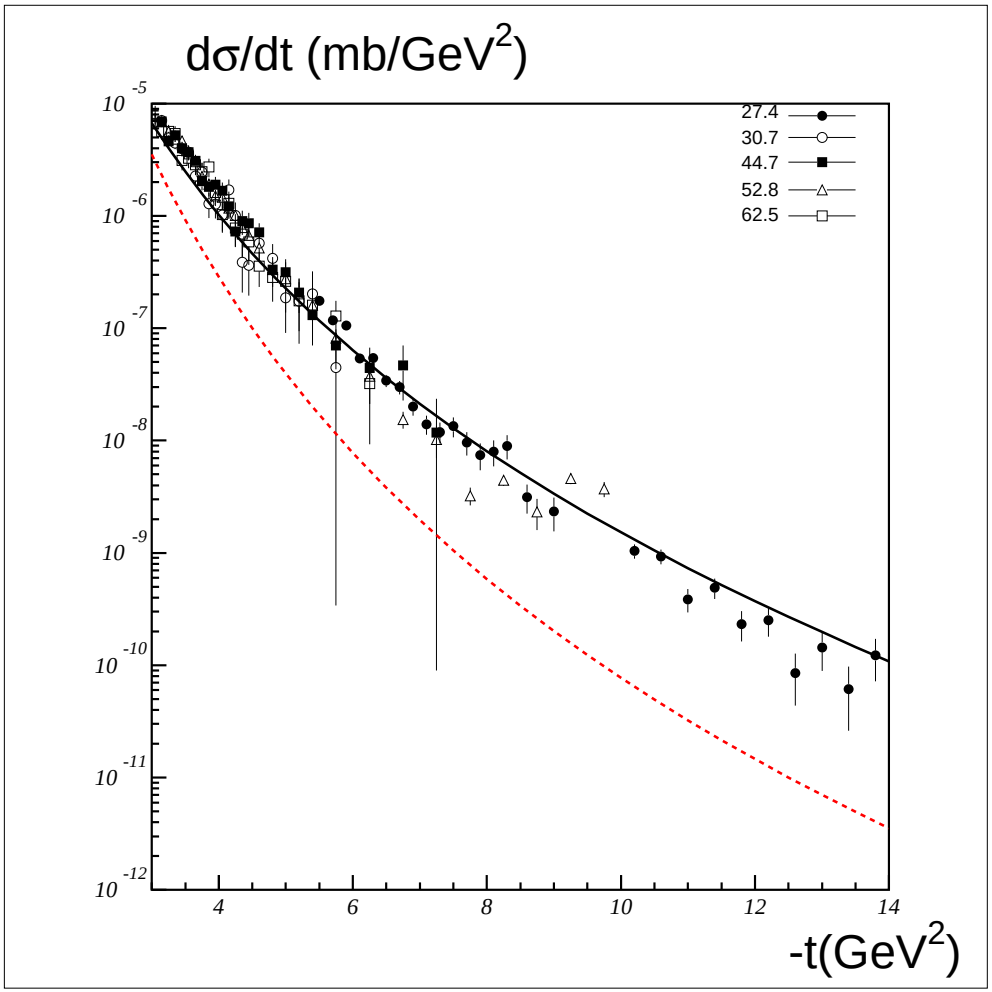

Figure 7: The contribution of pQCD exchange (dashed line) and AQCM contribution (solid line) to elastic proton-proton scattering at large energy and large momentum transfer.

Single-spin asymmetry A_N in PP and $P\bar{P}$ elastic scattering

$$A_N = -\frac{2Im[\Phi_5^*(\Phi_1+\Phi_2+\Phi_3-\Phi_4)]}{\mid\Phi_1\mid^2+\mid\Phi_2\mid^2+\mid\Phi_3\mid^2+\mid\Phi_4\mid^2+4\mid\Phi_5\mid^2},$$

where helicity amplitudes $\Phi_1 =< ++ \mid ++ >$, $\Phi_2 =< ++ \mid -- >$, $\Phi_3 =< +- \mid +- >$, $\Phi_4 =< ++ \mid -- >$ and $\Phi_5 =< ++ \mid -+ >$.

- **Spin-flip dominance in Odderon amplitude: $\Phi_5 =< ++ \mid -+ >$ amplitude is very large.**

- **Due to spin-flip the contribution of Odderon to the difference of PP and $P\bar{P}$ differential cross sections at $-t = 0$ is zero at high energies!**

- **Interference with spin-flip part of Pomeron amplitude at large $-t$. Difference in PP and $P\bar{P}$ cross sections in dip region $-t \sim 1-2$ GeV**

- **Large asymmetry A_N in PP and $P\bar{P}$ elastic scattering with**

opposite sign between them! The opposite sign for A_N in elastic $P\bar{P}$ can be checked at FAX Collaboration at FAIR.

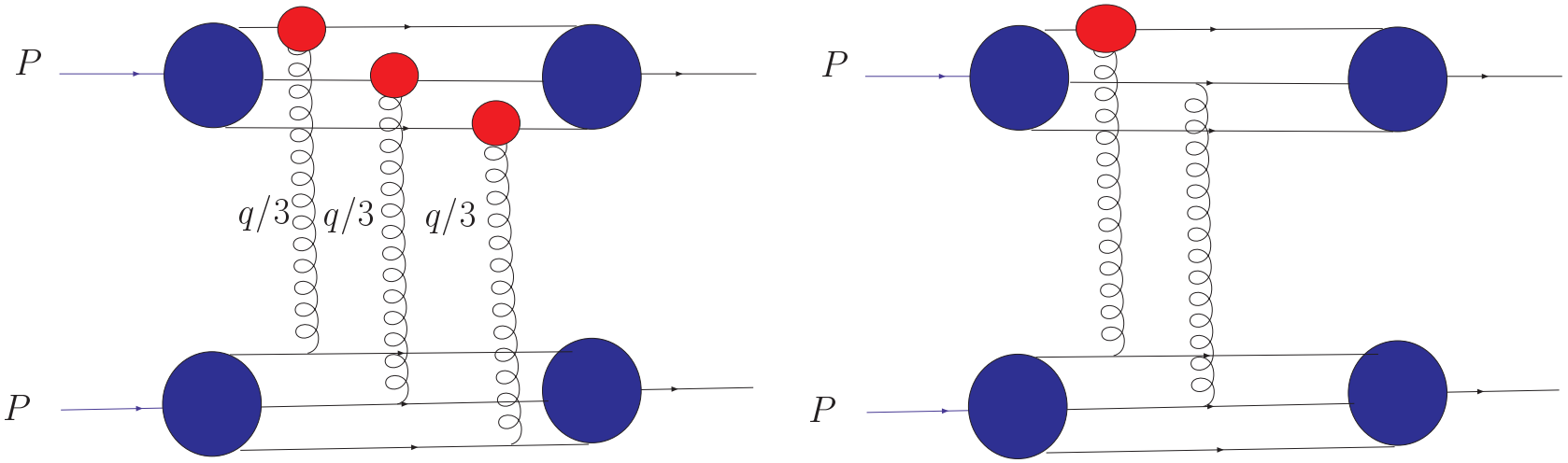

Figure 8: The interference between Landshoff-type AQCM diagram and pomeron spin-flip induced by AQCM.

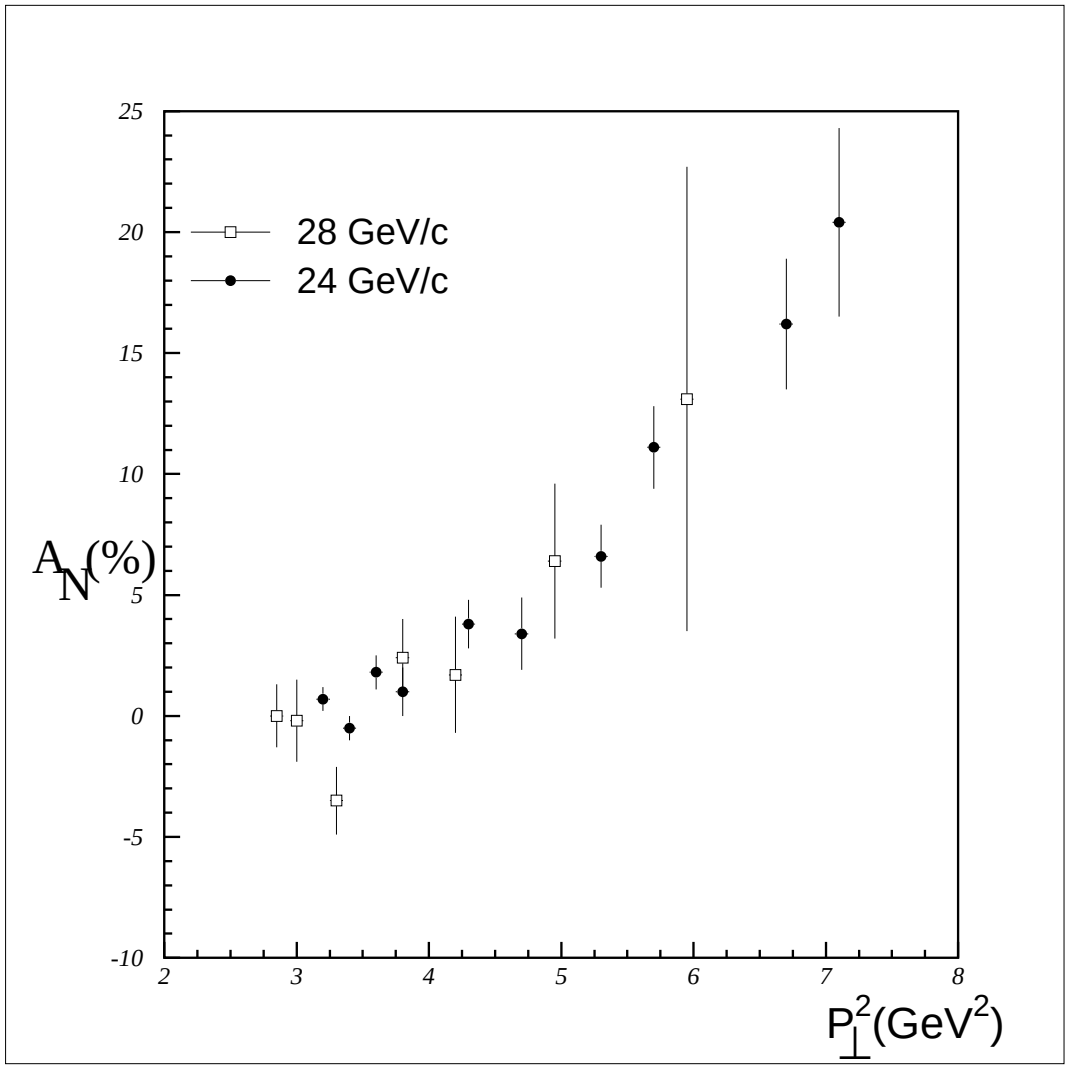

Figure 9: Single-spin asymmetry in the elastic $PP \to PP$ scattering at large momentum transfer at AGS.

"Direct" meson production induced by the instanton gluon fields

• Problem: perturbative QCD fails to describe the data for the high energy inclusive pion production in fixed target experiments (ISR, Fermilab data)

The AQCM related Lagrangian for anomalous pion production (APP) was introduced by N. K., Hee-Jung Lee, Baiyang Zhang, Pengming Zhang in Phys.Rev.D 92,034025(2015)

$$\mathcal{L}_{\pi qqg} = \frac{3\pi^2\rho_c^2}{4g_s(\rho_c)} g_{\pi qq}\overline{q}\sigma^{\mu\nu}t^a\gamma^5\tau\cdot\phi_\pi q G^a_{\mu\nu}, \qquad (1)$$

where, $\rho_c \approx 0.3$ fm is instanton size, the $g_s(\rho_c)$ is the strong coupling constant and $g_{\pi qq} = M_q/F_\pi$ is pion-quark coupling constant.

It was shown that the APP mechanism gives the dominated contribution to the high energy inclusive pion production at large Feynman x_F (at large rapidities) and in the few GeV region for the transverse momentum of the pion.

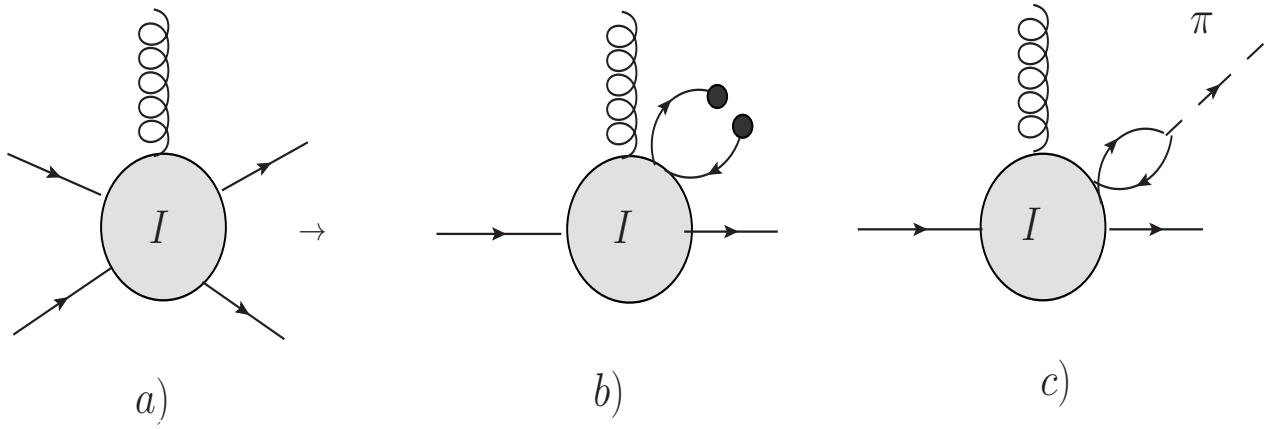

Figure 10: The diagram a) presents the general quark-gluon vertex generated by instantons for $N_f = 2$ case , b) corresponds to the case with one of the quark lines connected through the quark condensate, and c) describes the direct production of the pion from the instanton.

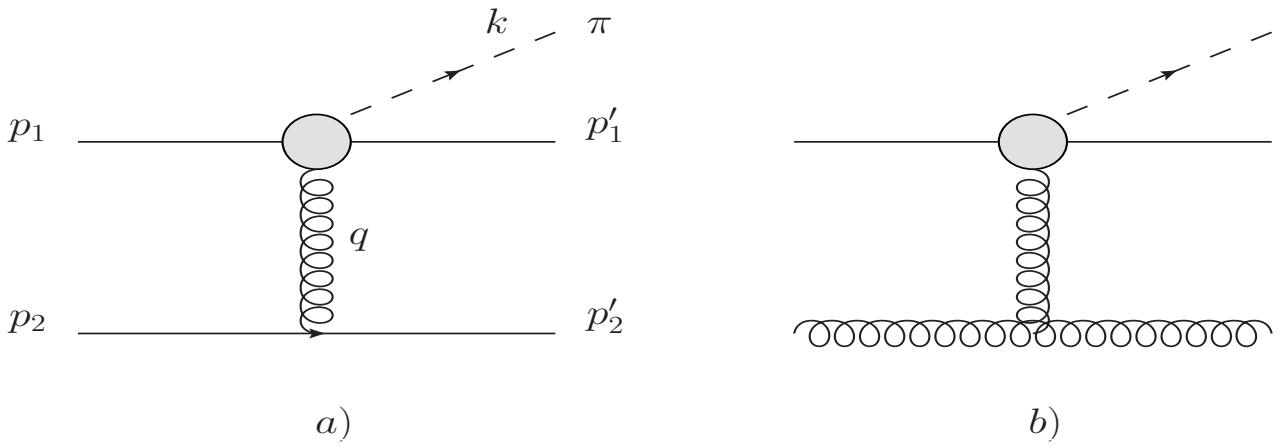

Figure 11: The pion production induced by instanton a) in quark-quark scattering and b)in quark-gluon scattering.

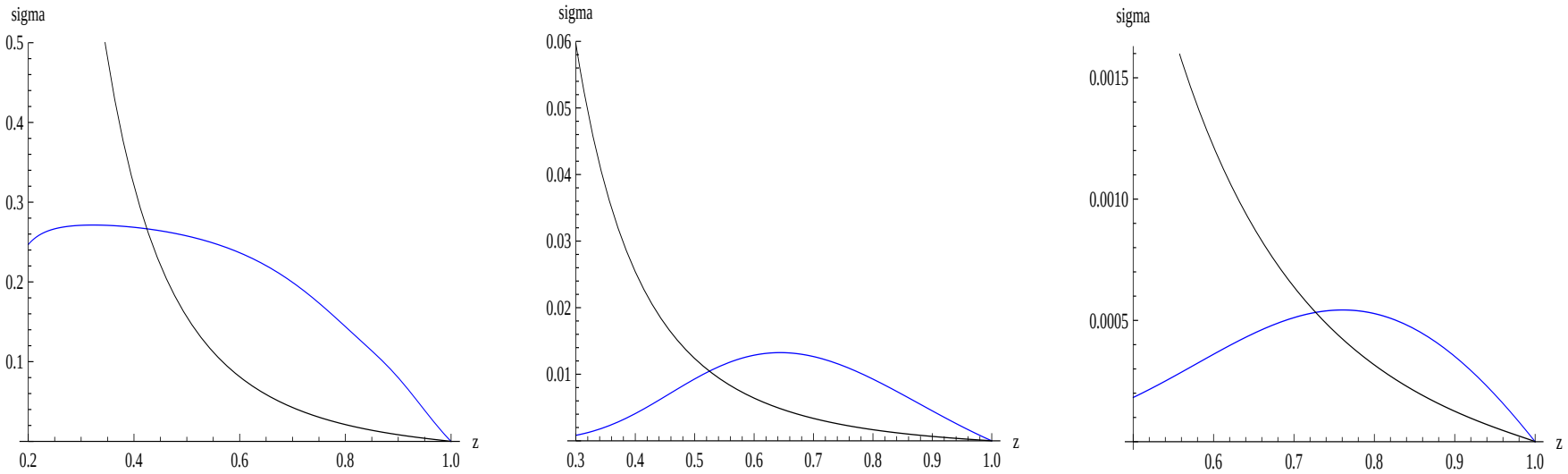

Figure 12: The z dependency of the pQCD (black line) and the APP (blue line) cross sections, in the units $10^2 \mu b/GeV^2$, for the different values of the pion transverse momentum: the left panel $k_t = 1$ GeV, the central panel $k_t = 2$ GeV, and the right panel $k_t = 3$ GeV. Here, the relation $k_t = |\vec{k}| \approx \sqrt{-q^2}$ was used. The z is the part of initial momentum of quark carried by the final pion.

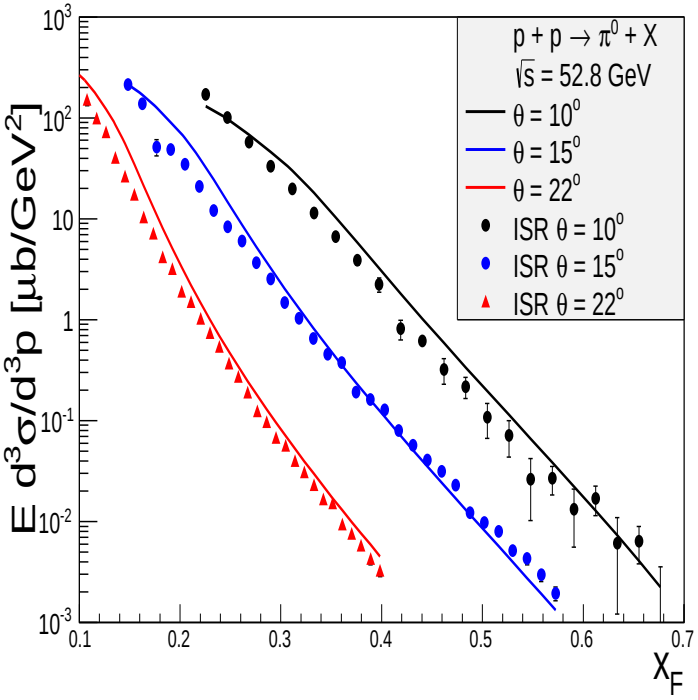

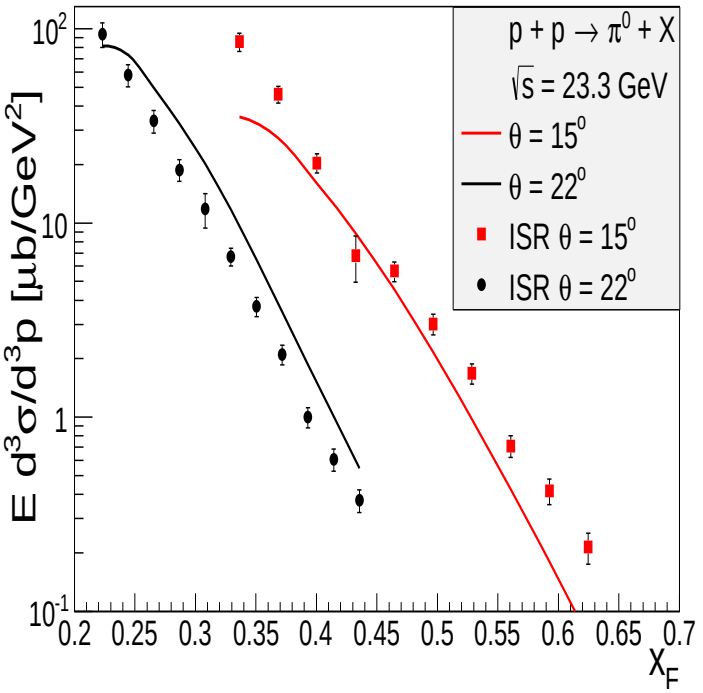

Figure 13: The APP cross sections for inclusive π^0 in comparison with the ISR fixed target data.

- Should the same mechanism give the important contribution to the another high energy reactions?

Nonperturbative energy loss by fast parton in strongly interacted Quark-Gluon Plasma

• Strongly interacted Quark-Gluon Plasma (sQGP) is produced at high energy heavy ion collision (current accelerators RHIC, LHC and future FAIR (GSI) and NICA (JINR)).

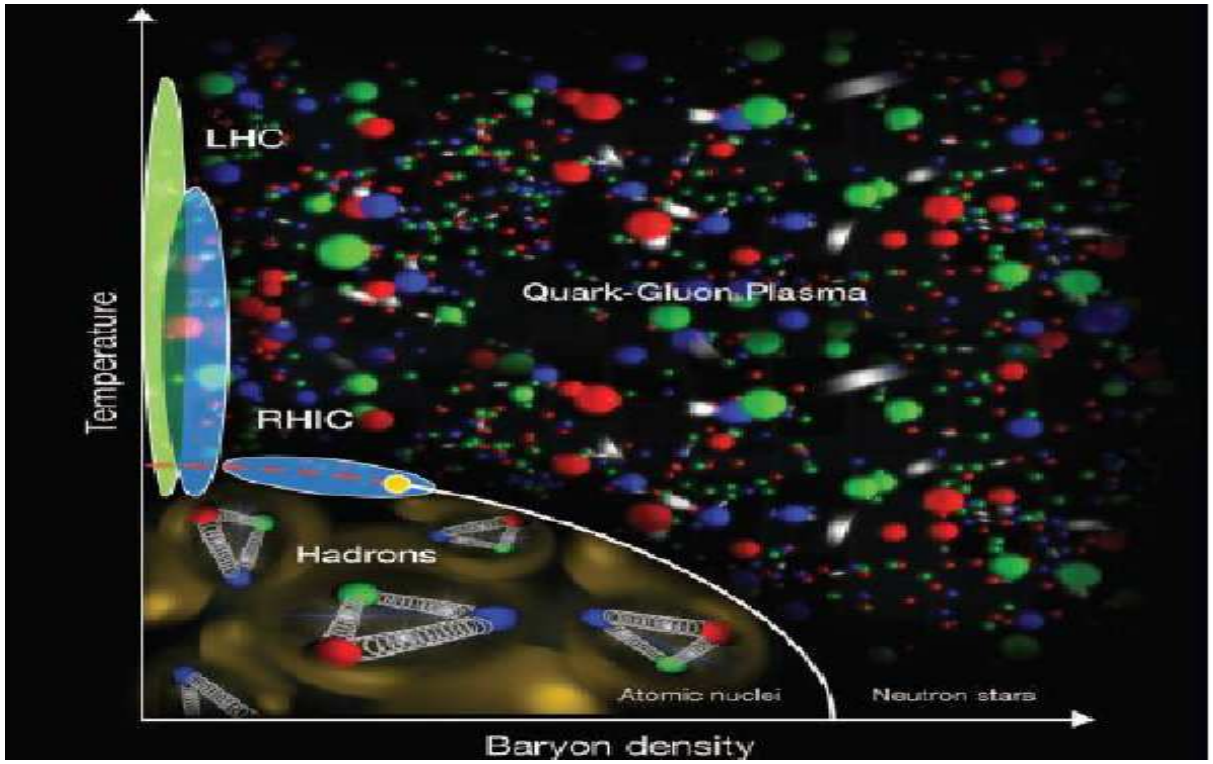

Figure 14: Phases in high energy heavy ion collisions

QCD phase diagram - prospects for NICA

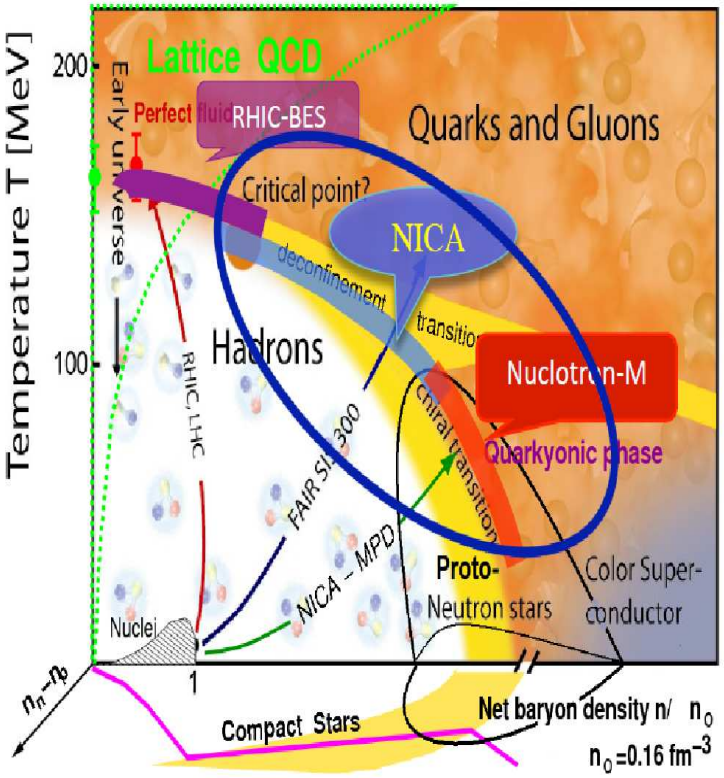

Energy Range of NICA is unexplored region of the QCD phase diagram:

- Highest net baryon density
- Onset of deconfinement phase transition
- Strong discovery potential:
  - a) Critical End Point (CEP)
  - b) Chiral Symmetry Restoration

NICA experimental programme is complementary to the RHIC/BES, FAIR and CERN and can be started already at Nuclotron-M

So, the NICA facilities provide unique capabilities for studying a variety of phenomena in a large region of the phase diagram

Figure 15: Phases in heavy ion collisions-detailes

• Secondary particle production suppression factor and jet quenching as a tool for investigation of the Quark-Gluon Matter created in high energy heavy ion collision.

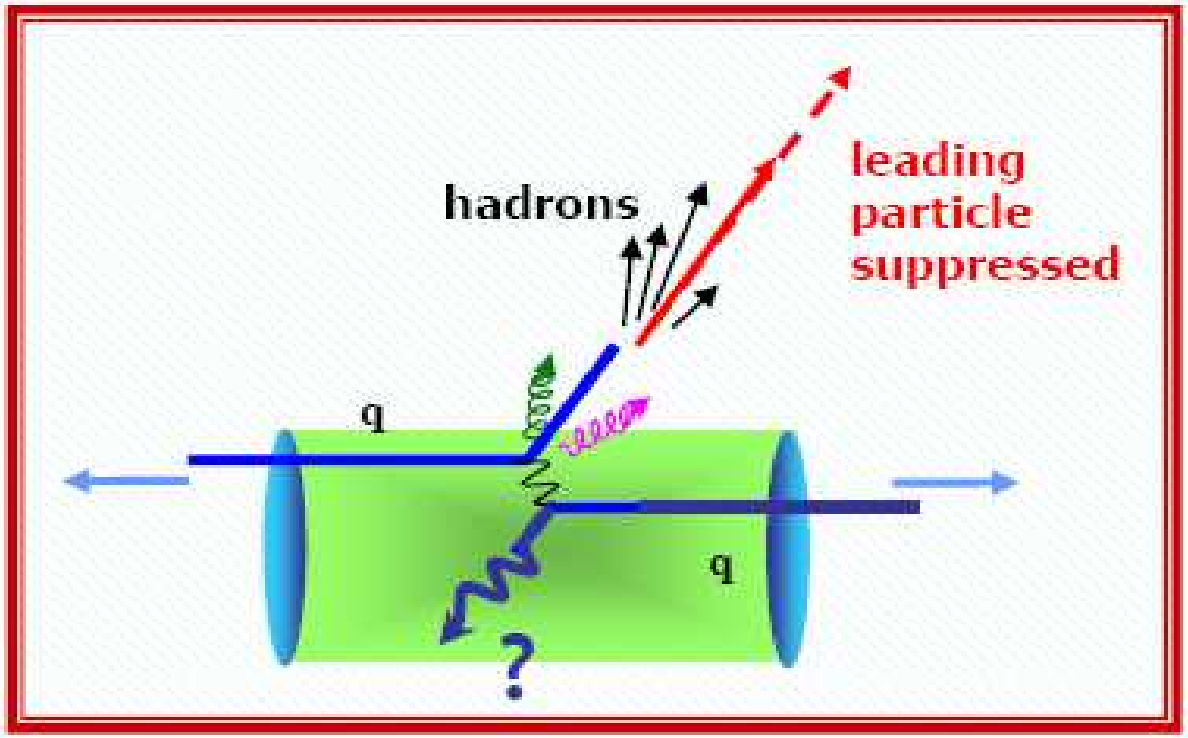

Figure 16: Nuclear modification factor

The nuclear modification factor

$$R_{AA}(p_\perp) = \frac{dN(A+A \to h+X)/dp_\perp dy}{< T_{AA} > d\sigma(N+N \to h+X)/dp_\perp dy}$$

where $< T_{AA} >$ is nuclear overlaping function which is the ratio of the number of the binary nucleon-nucleon collisions, $N_{coll} >$, calculated in Glauber model.

• The important RHIC and LHC heavy ion results are the observation of the strong secondary particle suppression and jet quenching coming from the interaction of the energetic quark or gluon with Quark-Gluon Matter.

• Perturbative contribution (radiative and elastic) is rather small and need to introduce very dense gluon matter to produce sufficient suppression. Additional problem is to describe a large heavy quark jet quenching.

• In spite of the fact that density of produced QGP at LHC ($dN_g/dy \approx 2000 - 4000$ in Pb-Pb collision at $\sqrt{s_{NN}} = 2.76$ GeV)is about factor twice larger than at RHIC ($dN_g/dy \approx 1000 - 1400$ for Au-Au collision at $\sqrt{s_{NN}} = 200$ GeV) experiments at LHC show that the nuclear modification factor is approximately the same as at RHIC. Furthermore,

for heavy quarks it is about $R_{AA}^{c/b} \approx 0.5$ at $p_\perp > 3$ GeV at LHC in comparison with $R_{AA}^{c/b} \approx 0.2 - 0.3$ at RHIC.
See recent paper by Horowitz and Gyulassy Nucl.Phys. **A872** (2011) 265 "The surprising transparent sQGP at LHC"

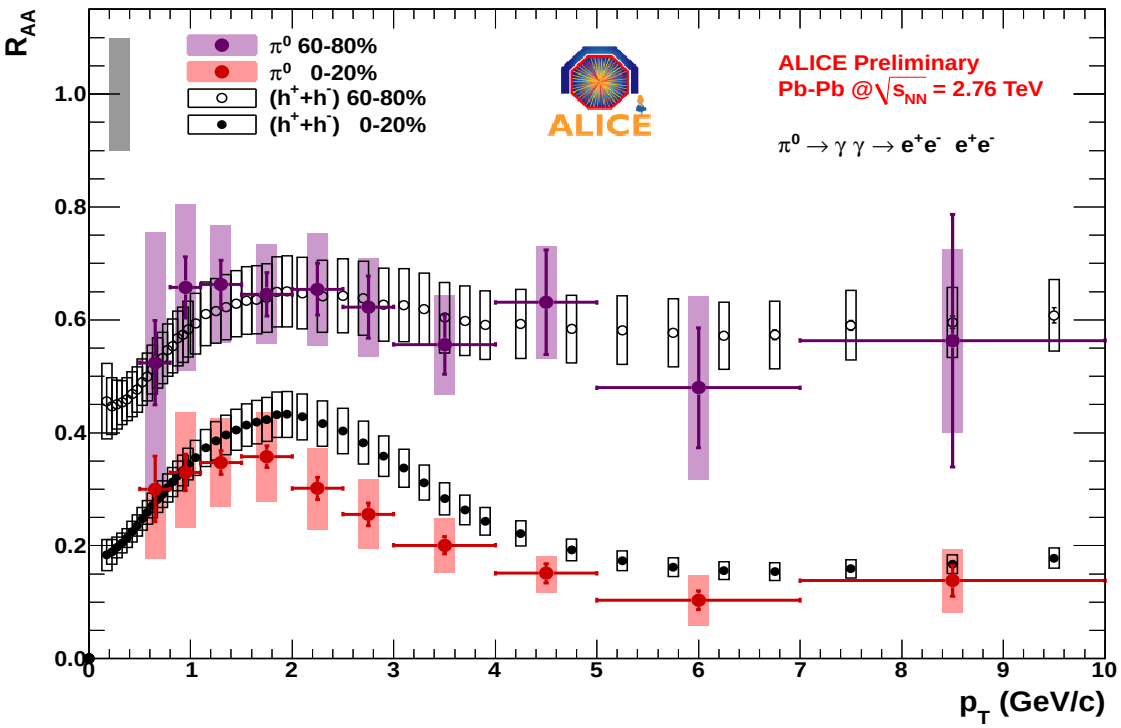

Figure 17: R_{AA} suppression factor at LHC.

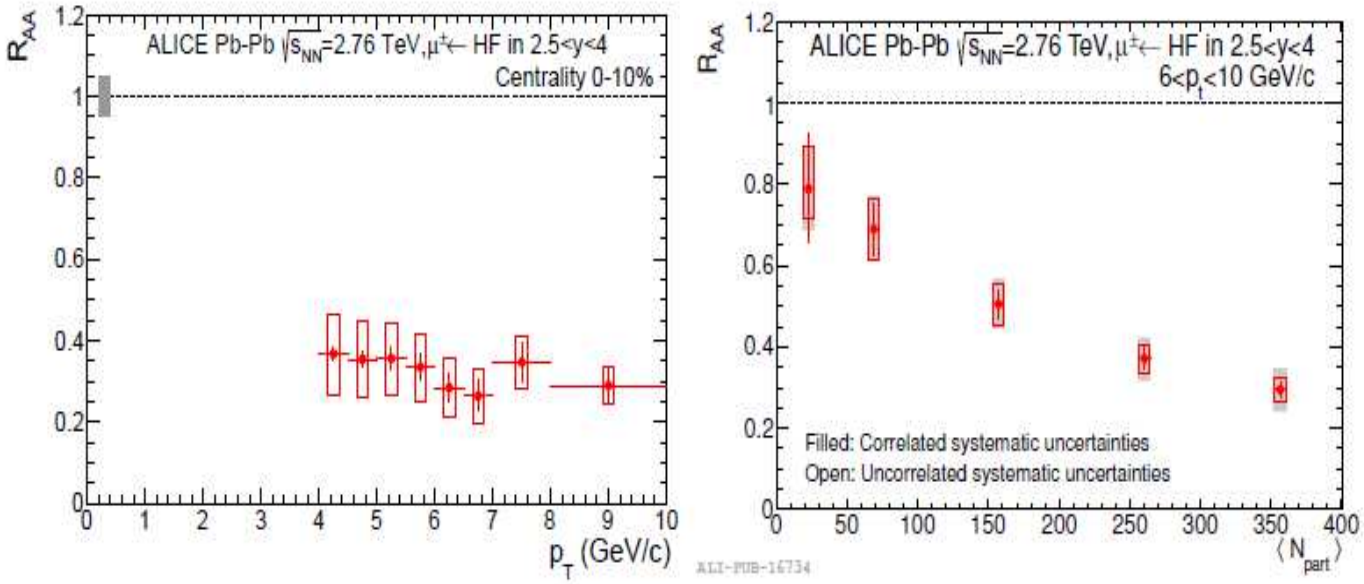

Figure 52: Nuclear modification factor R_{AA} of heavy-flavour decay muons with $2.5 < y < 4$ measured in Pb–Pb collisions at $\sqrt{s_{NN}} = 2.76$ TeV as a function of p_T in the 10% most central collisions (left panel) and as a function of the mean number of participating nucleons $\langle N_{part} \rangle$ (right panel) [117].

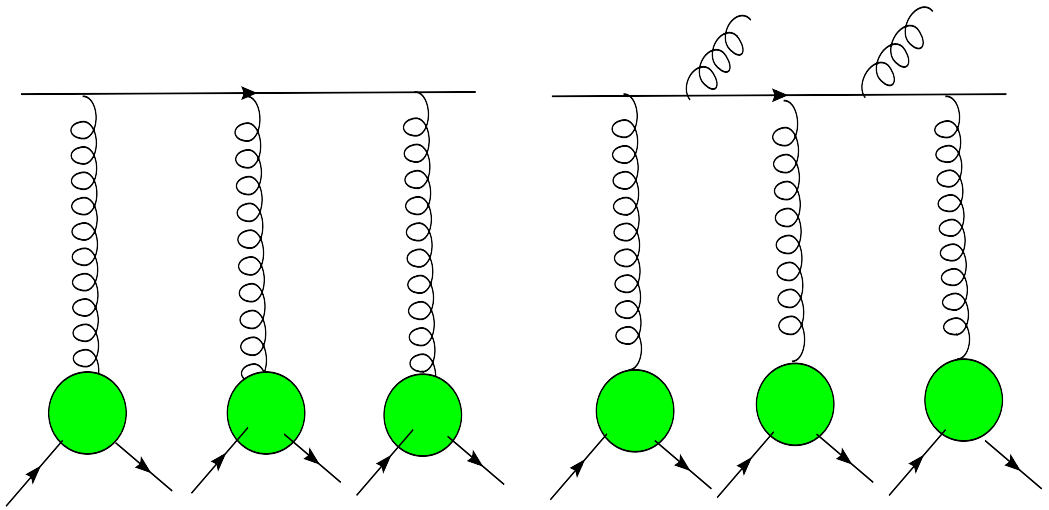

Figure 18: The pQCD a) elastic and b) radiative energy losses.

Transport coefficient for energy loss

$$\hat{q} = \rho \int t \frac{d\sigma}{dt} dt$$

For cold nuclear matter $\rho \approx 0.16$ fm^{-3} and

$$\hat{q}_{cold}^{pQCD} \approx \frac{3\pi^2 \alpha_s}{2} \rho [xG(x, Q^2]$$

For small x region $[xG(x)] \approx 1-2$ and we have got (Baier, Dokshitzer, Mueller et al NP, **B484** (1997) 265.)

$$\hat{q}_{cold}^{pQCD} \approx 0.05 - 0.1 GeV^2/fm$$

For hot QGP at $T \sim 300$ MeV for RHIC

$$\hat{q}_{hot}^{pQCD} \approx 1 GeV^2/fm$$

It is TOO SMALL to explain RHIC data!

Heavy quark non-perturbative energy loss by heavy quark induced by anomalous quark-gluon pion interaction

N. Kochelev, H. J. Lee, Y. Oh, B. Zhang and P. Zhang, "Nonperturbative collisional energy loss of heavy quarks in quark-gluon plasma," Phys. Rev. C **93**, no. 2, 021901 (2016) (Rapid Communication)

In formulas for energy loss the dominated contribution is coming from low transfer momentum region which is beyond validity of perturbative

QCD.
Therefore the calculation of energy loss should be done within *non-perturbative QCD framework*!

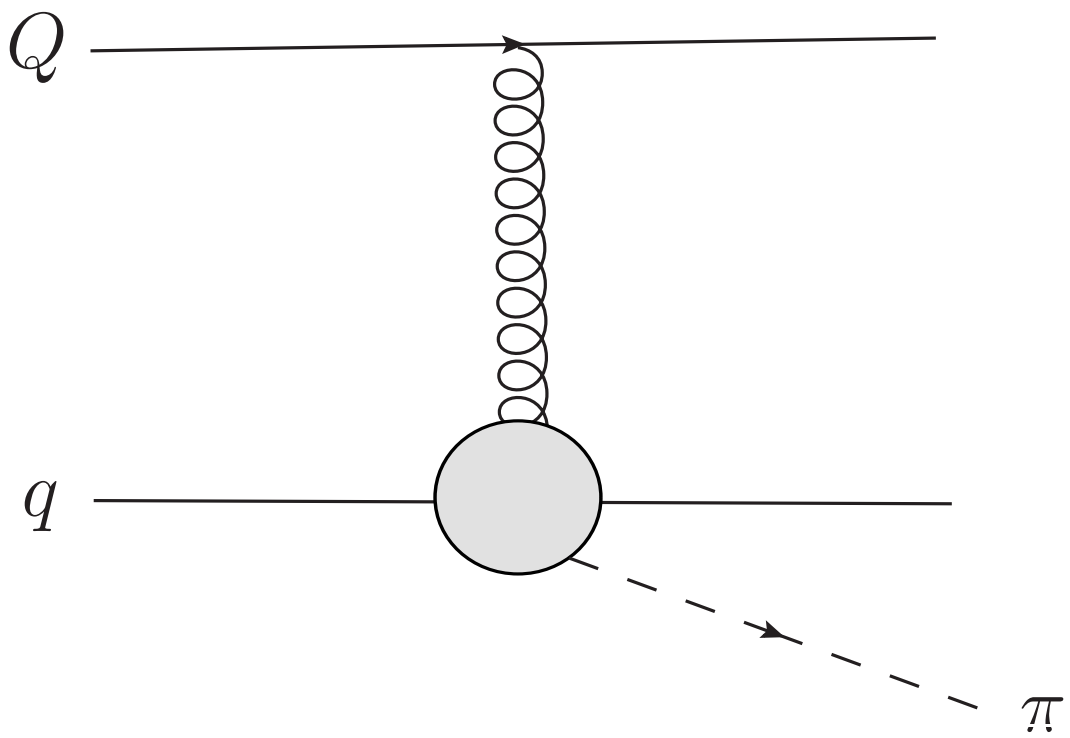

Figure 19: Diagram for heavy quark energy loss in QGP due to the quark-pion-gluon interaction. Here, Q and q stand for a heavy and a light quark, respectively. Produced pion has a very small size ~ 0.3 fm

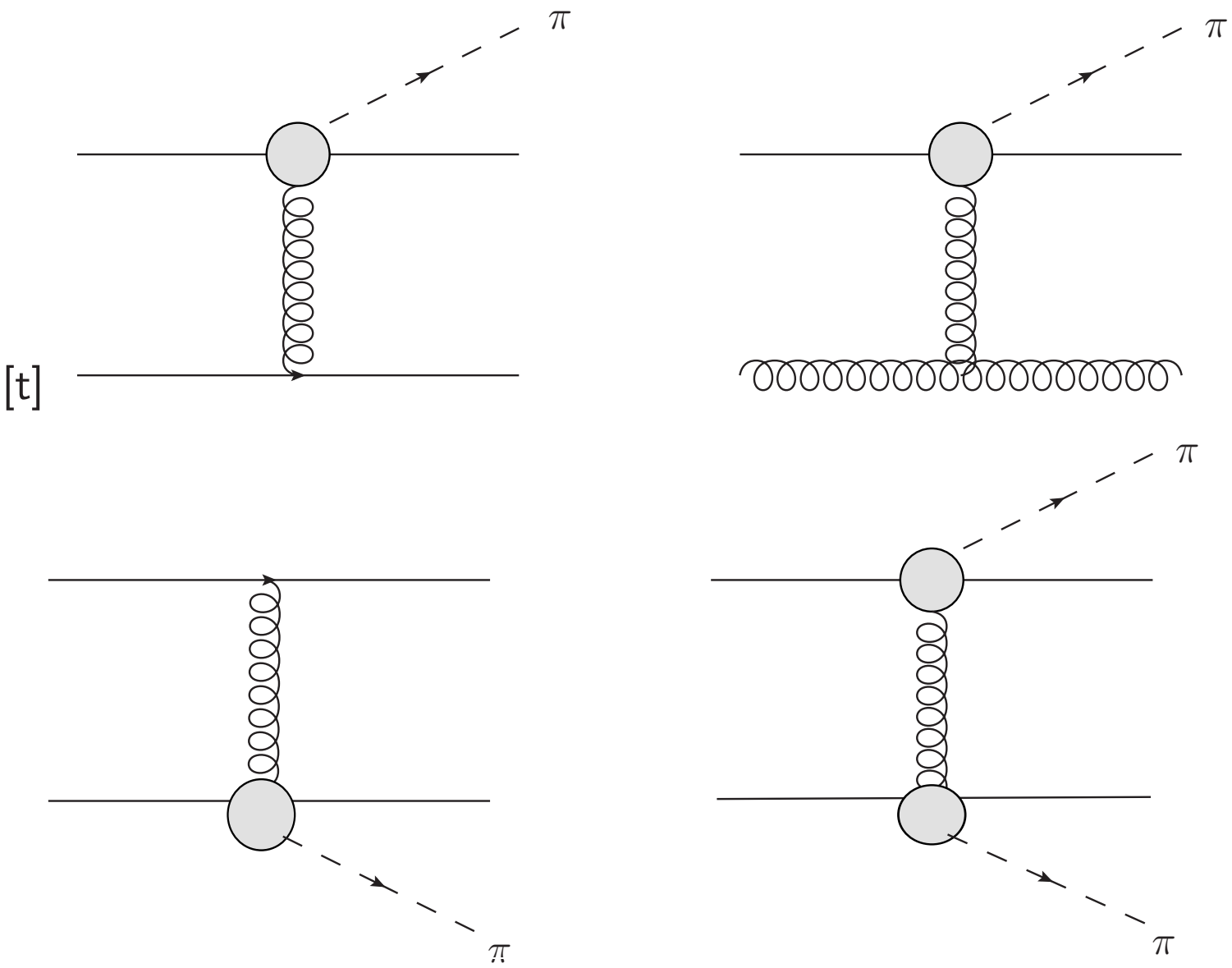

Diagrams which can contribute to the non-perturbative light quark energy loss in the QGP.

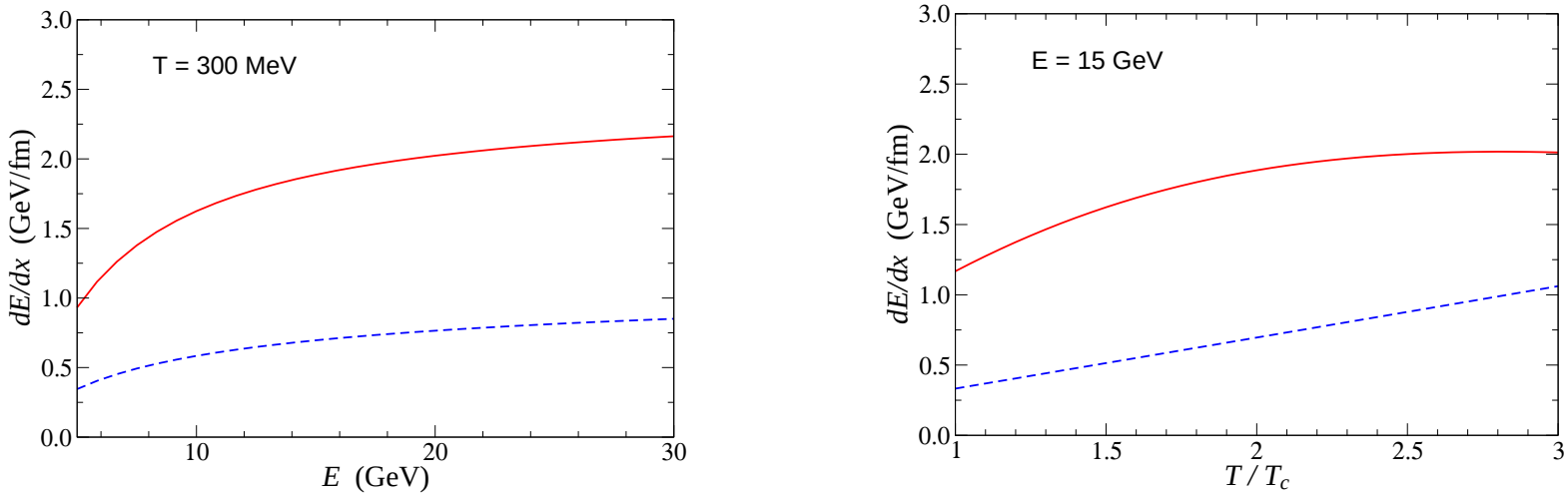

Figure 20: (a) The energy dependence of the non-perturbative (solid line) and perturbative (dashed line) collisional energy loss of a charm quark in QGP at $T = 2\,T_c$. (b) The temperature dependence of the energy loss at $E = 15$ GeV. The solid lines are the results from the nonperturbative calculation and the dashed lines are the perturbative results.

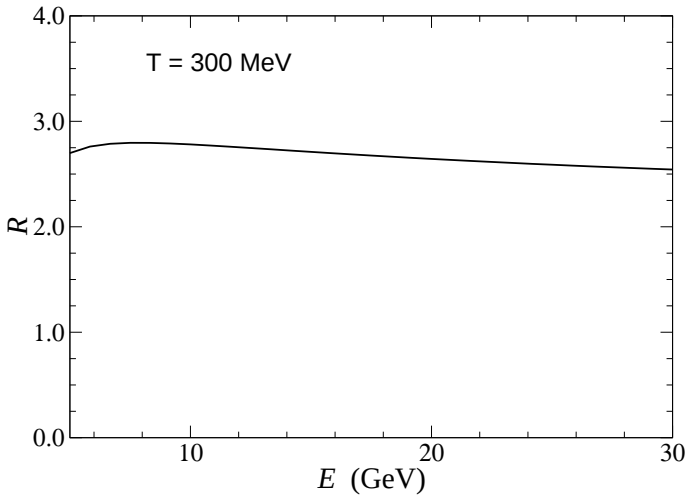

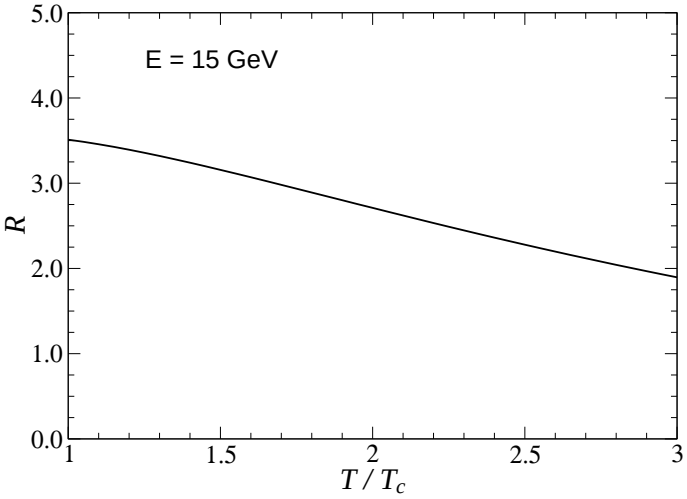

Figure 21: (a) The energy dependence of the ratio $\mathcal{R}$ of the non-perturbative to the perturbative contributions at $T = 2\,T_c$. (b) The temperature dependence of the ratio $\mathcal{R}$ at $E = 15$ GeV.

Very big non-perturbative contribution to the heavy quark energy loss in Quark-Gluon Plasma!

Instanton effects in the partonic distributions of nucleon: gluon distributions, spin and flavor structure of nucleon sea

Unpolarized and polarized gluon distributions inside the constituent quark and nucleon

N. Kochelev, H. J. Lee, B. Zhang and P. Zhang, "Gluonic Structure of the Constituent Quark," Phys. Lett. B **757**, 420 (2016)

The predictions for LHC experiments and for spin-dependent cross-sections at RHIC are very sensitive to the unpolarized and polarized gluon distributions. We are using DGLAP (Dokshitzer-Gribov-Lipatov-Altarelli-Parisi) approach to calculate the splitting functions coming from anomalous quark-gluon and quark-gluon-pion interactions and find out the probability to find gluon inside constituent quark with part of its momentum z.

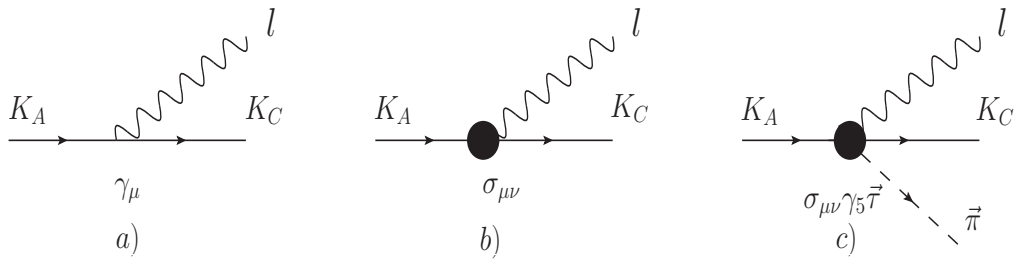

Figure 22: a) corresponds to the contributions from the pQCD to gluon distribution in the quark. b) and c) correspond to the contributions to the gluon distribution in the quark from the non-perturbative quark-gluon interaction and the non-perturbative quark-gluon-pion interaction, respectively.

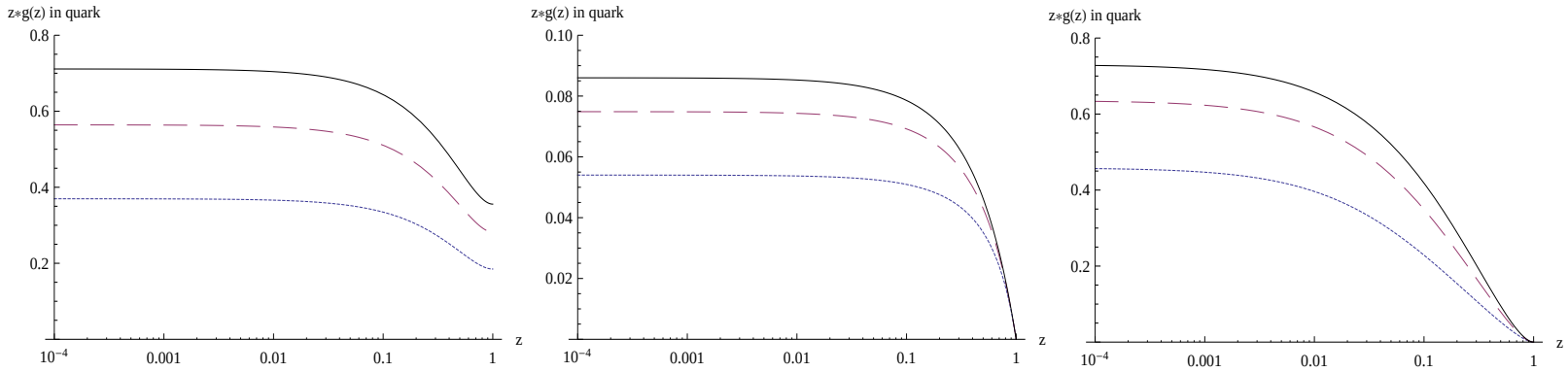

Figure 23: The z dependency of the contributions to the the unpolarized gluon distribution in the constituent quark from the pQCD (left panel), from the non-perturbative interaction without pion (central panel), and from the non-perturbative interaction with pion (right panel). The dotted line corresponds to $Q^2 = 2$ GeV^2, the dashed line to $Q^2 = 5$ GeV^2, and the solid line to $Q^2 = 10$ GeV^2.

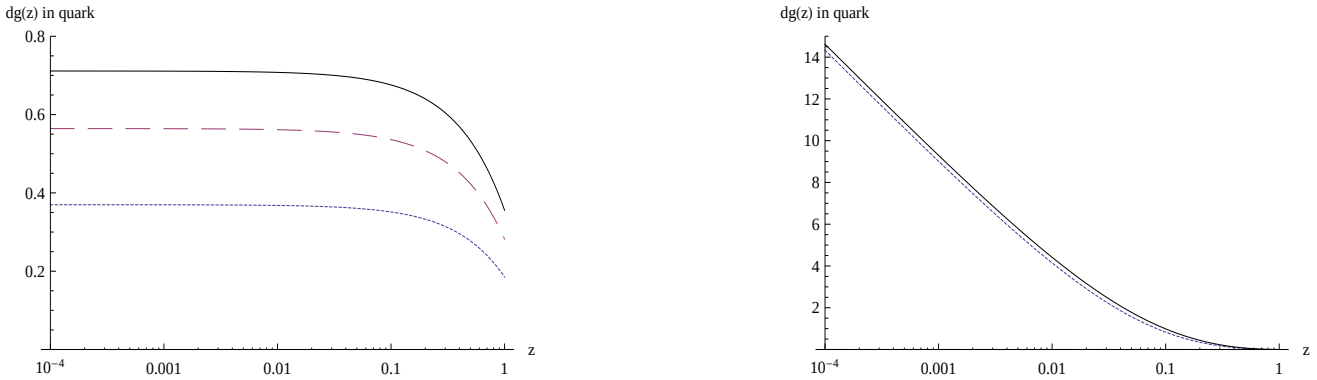

Figure 24: The z dependency of the contributions to the polarized gluon distribution in the constituent quark from the pQCD (left panel), and from the non-perturbative interaction with pion (right panel). The notations are the same as in the Fig.2. In the right panel the result for $Q^2 = 5$ GeV^2 does not shown because it is practically identical to the $Q^2 = 10$ GeV^2 case.

Gluonic distributions in the nucleon

We will apply the convolution model to obtain the gluon distributions in the nucleon from the gluon distributions in the constituent quark. It means that the probability to find gluon which carry the part of nucleon momentum xP is the product of the probability to find constituent quark with yP momentum inside nucleon and probability to find gluon inside constituent quark with definite momentum x/yP. Within this model the unpolarized and polarized gluon distributions in the nucleon are given by

$$
\begin{aligned}
g_N(x,Q^2) &= \int_x^1 \frac{dy}{y} q_V(y) g_q(\frac{x}{y},Q^2), \\
\Delta g_N(x,Q^2) &= \int_x^1 \frac{dy}{y} \Delta q_V(y) \Delta g_q(\frac{x}{y},Q^2),
\end{aligned}
$$

where $q_V(y)$ $(\Delta q_V(y))$ is unpolarized (polarized) distribution of constituent quark in the nucleon and $g_q(z,Q^2)$ $(\Delta g_q(z,Q^2))$ is the gluon distribution in the constituent quark obtained above. For the

unpolarized constituent quark distribution, we take

$$q_V(y) = 60y(1-y)^3.$$

At the large y this distribution is in accord with the quark counting rule. Its behavior in small y region and its normalization are fixed by the requirements $\int_0^1 dy q_V(y) = 3$ and $\int_0^1 dy y q_V(y) = 1$. It means that total momentum of nucleon at $Q^2 \to 0$ is carried by the three constituent quarks. For the polarized constituent quark distribution the simple form is assumed

$$\Delta q_V(y) = 2.4(1-y)^3.$$

This form is also in agreement with the quark counting rule at $y \to 1$. The normalization has been fixed from the hyperon weak decay data as

$$\int_0^1 dy \Delta q_V(y) = \Delta u_V + \Delta d_V \approx 0.6.$$

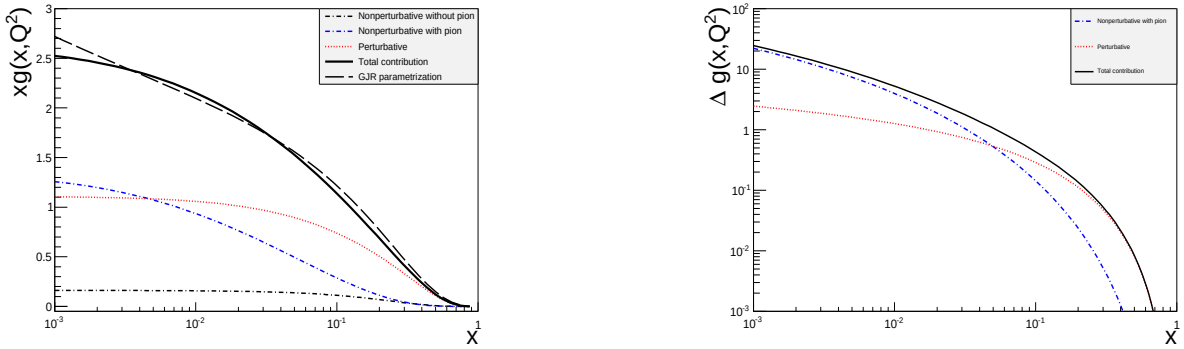

Figure 25: Unpolarized (left panel), and the polarized (right panel) gluon distributions in the nucleon at the scale $Q^2 = 2$ GeV^2. The dotted line in red corresponds to the contribution from pQCD, the dotted-dashed in blue to the contribution from the non-perturbative interaction with pion, dotted-dashed in black to the contribution from the non-perturbative interaction without pion, and the solid line to the total contribution.

"Spin Crisis": Where the Proton Spin is?

The famous proton spin problem is one of the longstanding puzzle in the QCD . The decomposition of the proton spin by Jaffe and Manohar is

$$\frac{1}{2} = \frac{1}{2}\Delta\Sigma + \Delta G + L_q + L_g,$$

where the first term is quark contribution, $\Delta G = \int_0^1 dx \Delta g(x)$ is the gluon polarization in nucleon and the last two terms are the contributions from the orbital motions of the quarks and the gluons. The main problem is how to explain very small value of the proton spin carried by quark. At the present, the typical value is $\Delta\Sigma(Q^2 = 2GeV^2) \approx 0.25$, which is far away from $\Delta\Sigma = 1$ given by the non-relativistic quark model. The relativistic motion of the quarks in the confinement region results in sizable decreasing of total helicity of quarks. For example, within the bag model one obtains $\Delta\Sigma = 0.65$. We should point out that this value is in agreement with the weak hyperon decay data, but it is not enough to explain the small value coming from deep inelastic scattering (DIS) at large $Q^2 \geq 1$ GeV^2. Just after appearance of the EMC data on the small part of the spin of the proton carried by the quarks, the axial anomaly

effect in DIS was considered as the primary effect to solve this problem . For the three light quark flavors, it gives the following reduction of the quark helicity in the DIS

$$\Delta\Sigma_{DIS} = \Delta\Sigma - \frac{3\alpha_s}{2\pi}\Delta G \tag{2}$$

It is evident that one needs to have a huge positive gluon polarization, $\Delta G \approx 3 \div 4$, in the proton to explain the small value of the $\Delta\Sigma_{DIS}$. The modern experimental data from the inclusive hadron productions and the jet productions exclude such a large gluon polarization in the accessible intervals of x and Q^2. Our model also exclude the large polarization of gluons (see Fig.5, right panel) in these intervals.

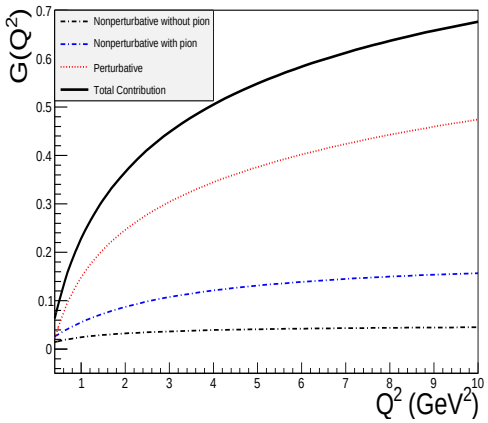

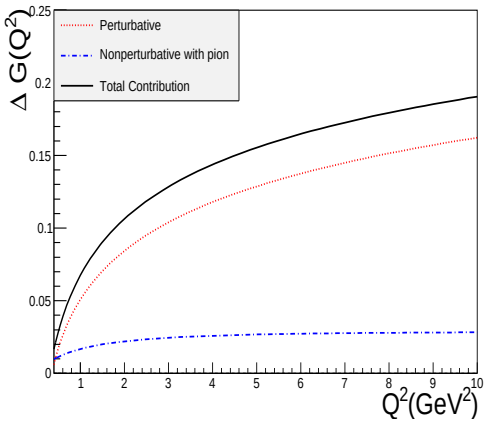

Figure 26: The part of the nucleon momentum carried by gluons (left panel), and the contribution of the gluons to nucleon spin (right panel) as the function of Q^2.

For example, at $Q^2 = 10$ GeV^2 the $\int_0^1 dx \Delta g(x) = 0.19$ in our model. This value is in agreement with recent fit of available data on spin asymmetry from the jet productions and the inclusive hadron productions.

Therefore, the axial anomaly effect, suggested by Efremov-Teryaev-Altarelli-Ross, cannot explain the proton spin problem.

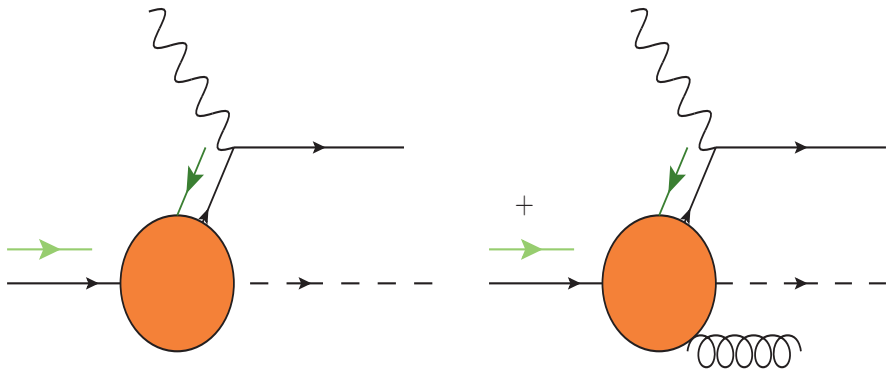

Figure 27: Quark depolarization induced by anomalous quark-gluon interaction. The green arrows are the direction of quark spin.

We should stress that the helicity of the initial quark is flipped in the non-perturbative vertices in Fig.7. As the result, such vertices should lead to the *screening* of the quark helicity. It is evident that at the $Q^2 \to 0$ such screening is vanished and the total spin of the proton is carried by its constituent quarks. Due to the total angular momentum conservation, for $Q^2 \neq 0$, the flip of the quark helicity by the non-perturbative interactions should be compensated partially by the orbital momenta of the partons and pion *inside* the constituent quark.

Flavor asymmetry of nucleon quark sea induced by instantons

A. E. Dorokhov and N. I. K. Phys. Lett. **B304** (1993) 167.

Gottfried sum rule violation

$$\int_0^1 \frac{[F_2^p(x)-F_2^n(x)]}{x}dx = \frac{1}{3}\int_0^1 \frac{[F_2^p(x)-F_2^n(x)]}{x}dx$$
$$= \frac{1}{3}\int_0^1 (u_V(x)-d_V(x))dx - \frac{2}{3}\int_0^1 (\bar{d}(x)-\bar{u}(x))dx$$

NMC Collaboration

$$\int_0^1 (\bar{d}(x)-\bar{u}(x))dx = 0.11 \pm 0.02$$

NA51 Collaboration

$$\bar{d} \approx 2\bar{u}, \quad < x > \approx 0.18$$

Instanton induced flavor asymmetry of sea $d_s \approx 2u_s$

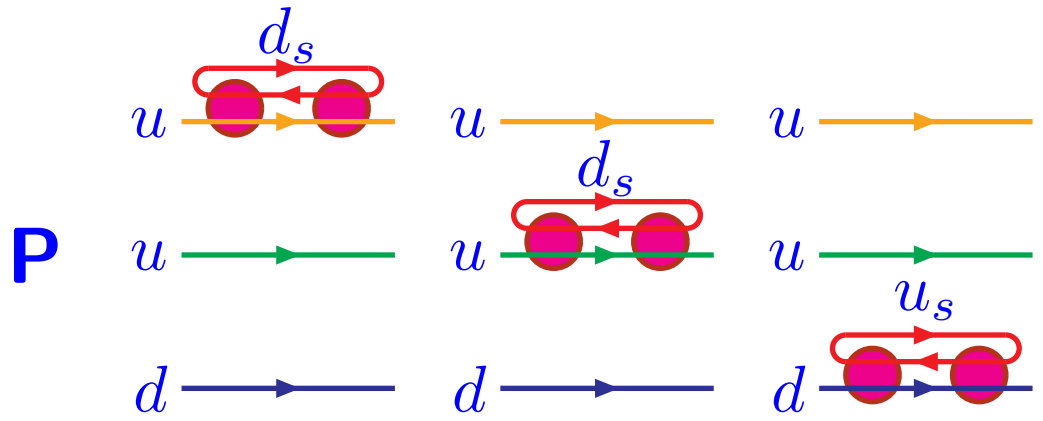

- **Connection between spin and flavor structure of proton sea**

$$\Delta\bar{u}(x) - \Delta\bar{d}(x) \approx \frac{5}{3}(\bar{d}(x) - \bar{u}(x))$$

Instantons and anomalous spin effects in strong interaction

N. Kochelev and N. Korchagin, "Anomalous Quark Chromomagnetic Moment and Single-Spin Asymmetries," Phys. Lett. B **729**, 117 (2014)

Single-spin asymmetries in high energy reactions

In perturbative QCD single-spin asymmetries are expected to be very small

$$A_N \approx \frac{\alpha_s m_{curr}}{p_\perp}$$

Large single-spin asymmetries were observed in many hadron reactions

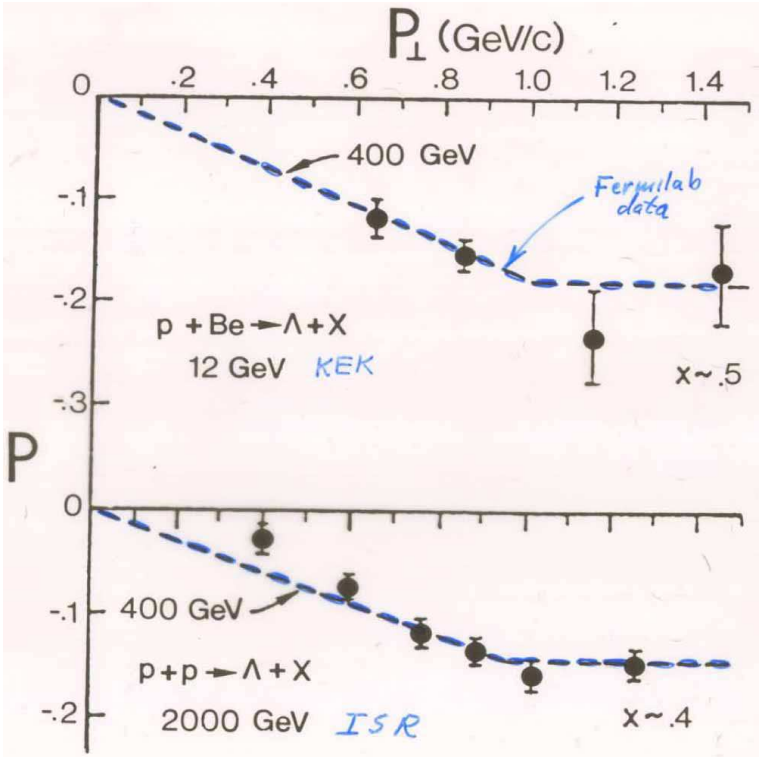

Figure 28: Λ polarization in unpolarized proton-proton and proton-nucleus collitions (from A.D.Krisch, arXiv:1001.0790).

Different mechanisms, mainly based on the factorization, have been suggested: twist-3 (Efremov, Teryaev), Sivers distribution and Collins fragmentation functions etc.

• Such approaches usually include many parameters which obtained by the fitting of the experimental data. Therefore their predictable

power is difficult to estimate.

- **Additional problem in these approaches is in the sign of SSA mismatching between proton-proton and SIDIS data.**

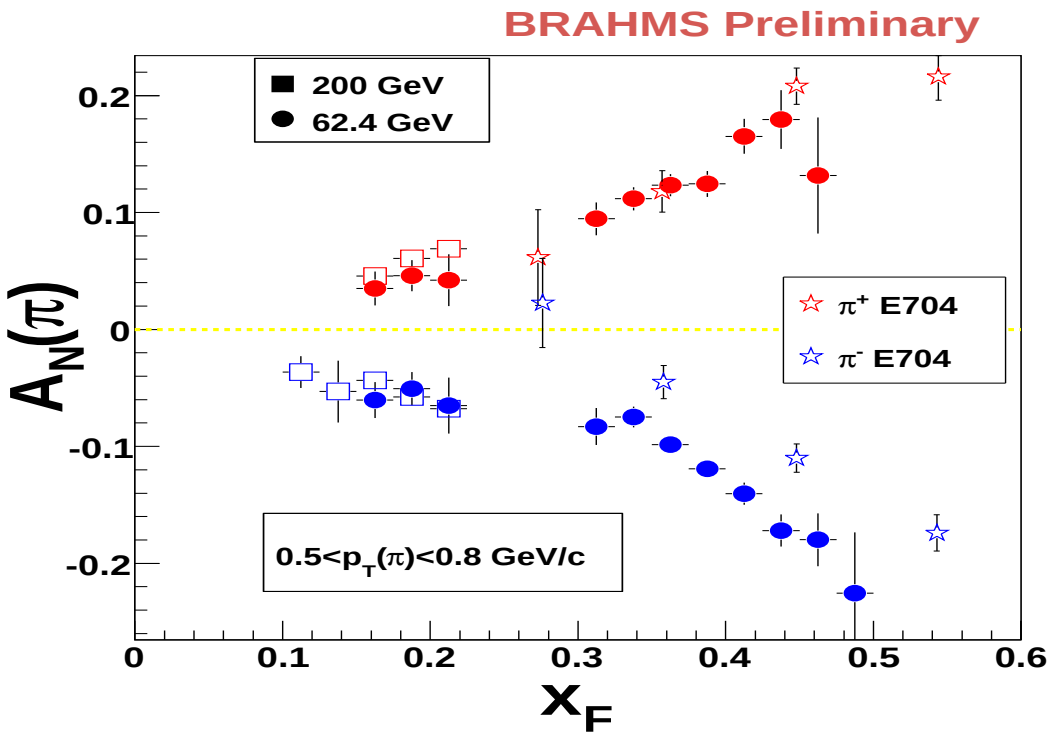

Figure 29: Comparison of charged pion asymmetries measured at 200 and 62.4 GeV by the BRAHMS experiment and at 19.4 GeV by the E704 experiment.

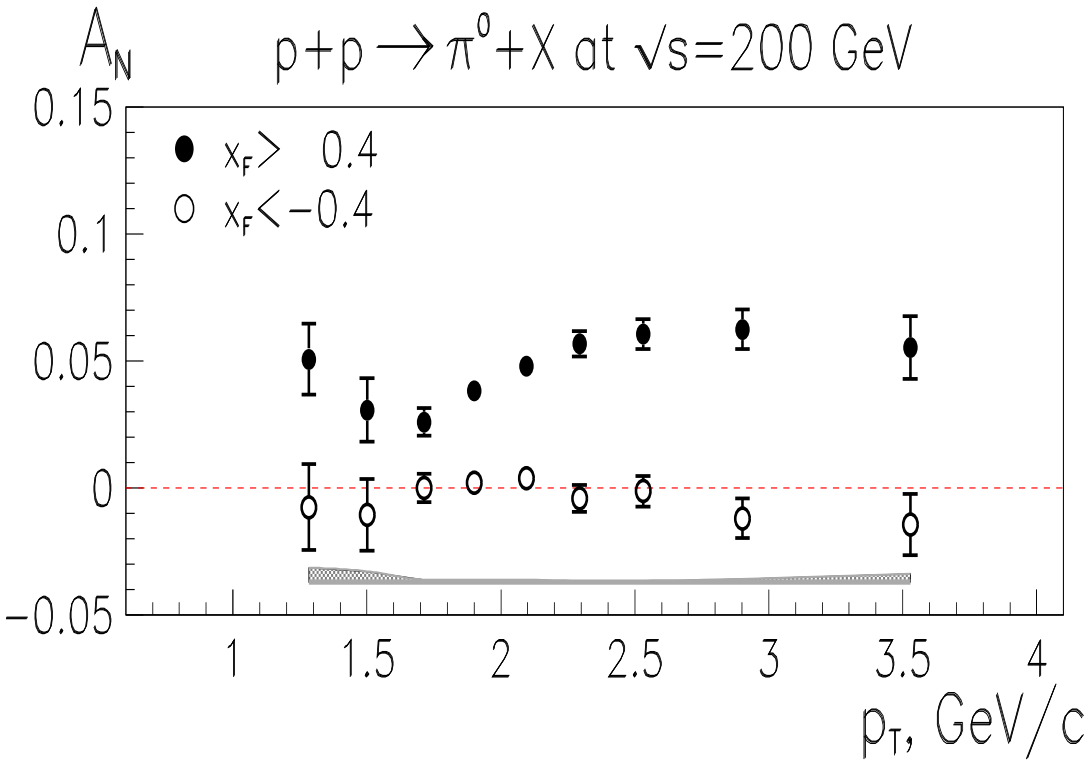

Figure 30: STAR experiment SSA data at $\sqrt{s} = 200$ GeV for neutral pions as the function of $P_{h\perp}$.

PHENIX and STAR data on π^0 and η SSA

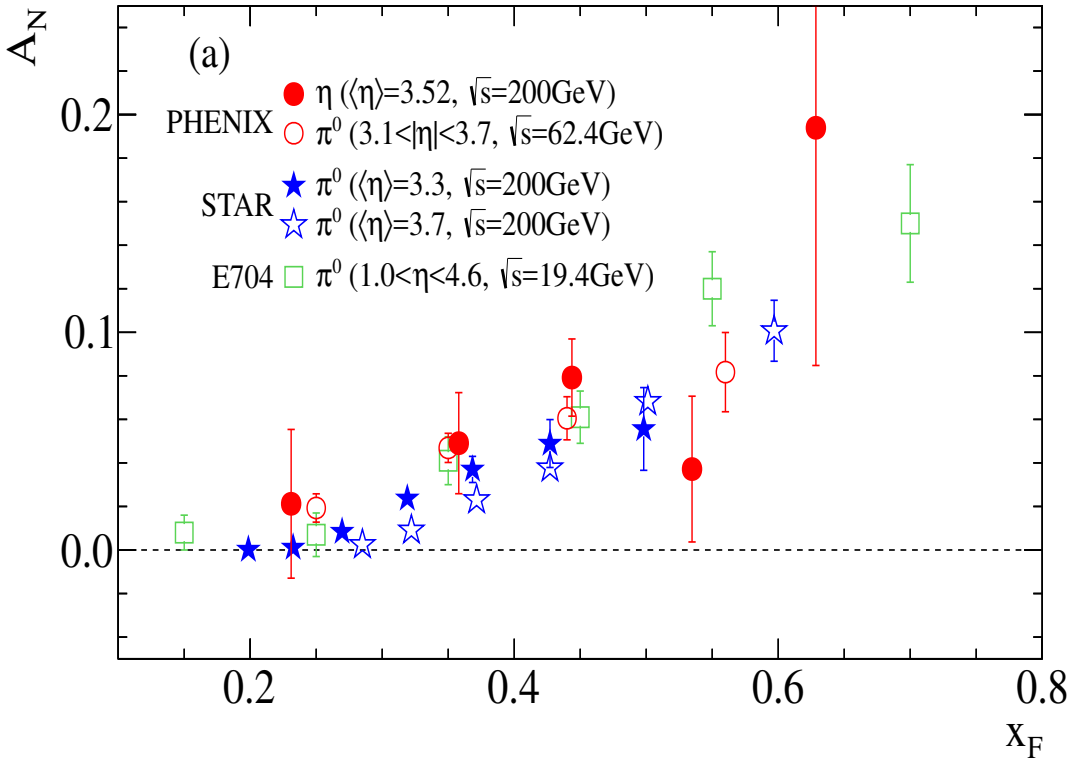

Figure 31: PHENIX and STAR SSA data at $\sqrt{s} = 200$ GeV for neutral pions and η-mesons as the function of x_F in comparison with the E704 data at $\sqrt{s} = 19.4$ GeV .

- Large asymmetry for η meson !
- Large negative SSA for neutron production (about 10%) at large

$x_F \to 1$ and small $p_T < 100$ MeV was observed by PHENIX Collaboration at RHIC at $\sqrt{S} = 200GeV$. Very strange nuclear dependency was observed as well. Result from $\pi - A_1$ interference (Kopeliovich at el) plus photon exchange ?

Baryon's SSA induced by quark-gluon chromomagnetic interaction

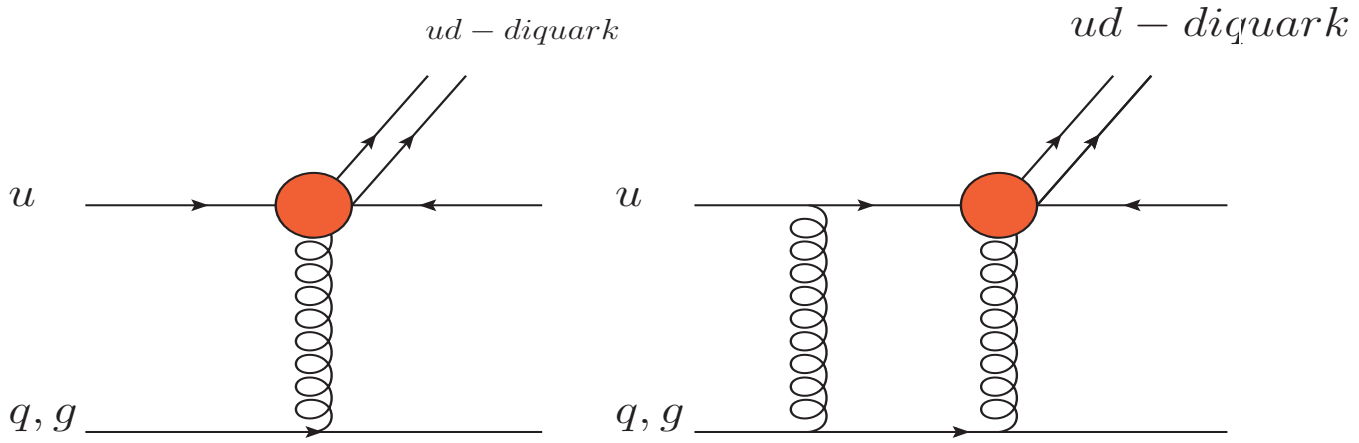

Figure 32: The diagrams which give the contribution to SSA of baryons, for example, proton,neutron and Λ .

AQCM and single-spin asymmetries

- Two important ingredients should be in the game to explain a large

single-spin asymmetries: large spin-flip amplitude and large imaginary part of non-spin-flip amplitude.

• Both of them have a natural origin coming from large AQCM. The sign of single-spin asymmetry is fixed by the sign of AQCM !

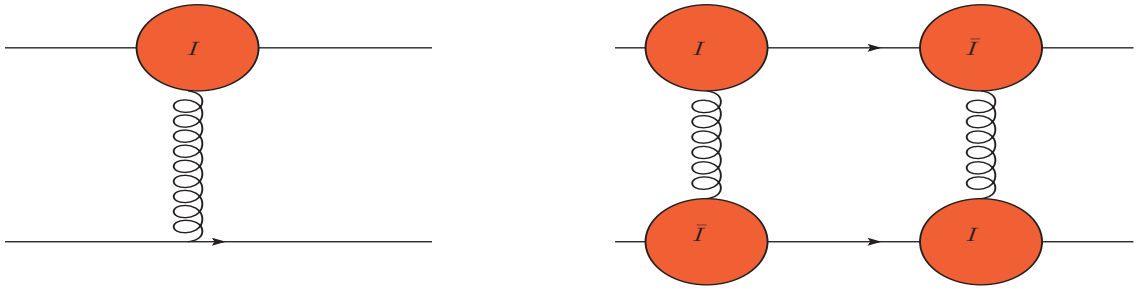

Figure 33: AQCM factorizable contribution to low $p_\perp$ high twist single-spin asymmetry in quark-quark scattering.

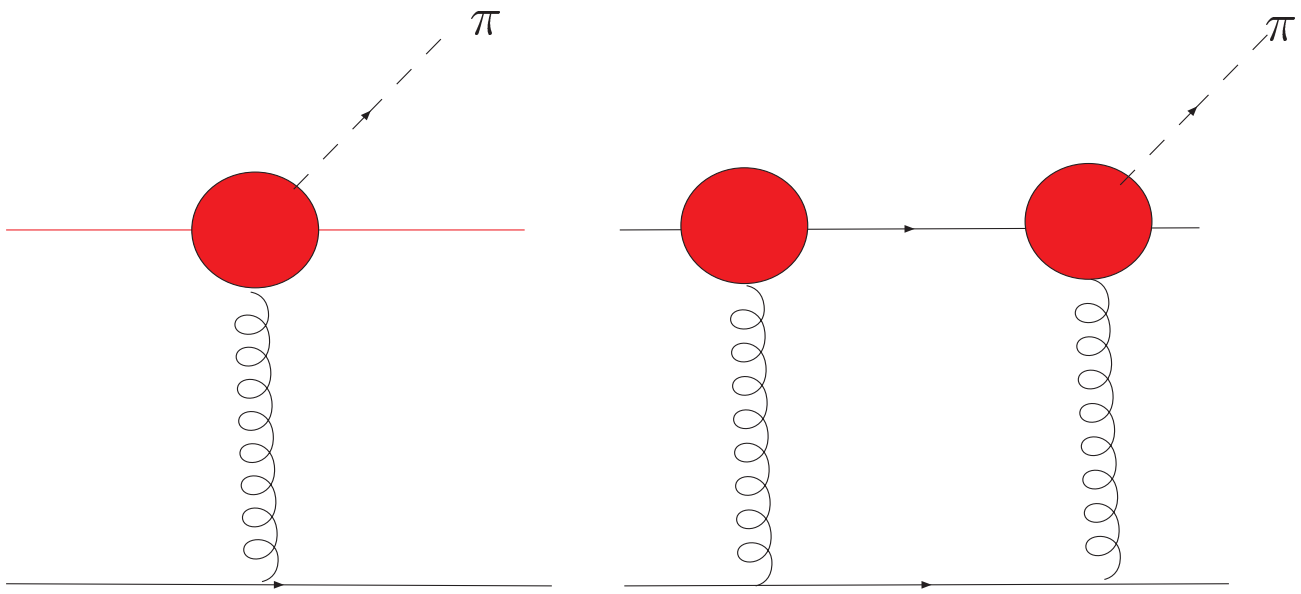

Figure 34: AQCM nonfactorizable contribution to large $p_\perp$ single-spin asymmetry for inclusive pion production in quark-quark scattering.

Conclusion

- **Instantons induce very specific quark-quark, quark-gluon and quark-gluon-pion interactions**

- **These interactions give an important contribution to the hadrons properties and to the reactions at high energy with hadrons**

- **It gives the fundamental QCD mechanism for the explanation of anomalous large spin and flavor effects in hadron physics**

Thank you very much for your attention!